

# **SANDIA REPORT**

SAND2007-7045

Unlimited Release

Printed October 2007

## **Low Inductance Gas Switching**

Chuck Harjes, Juan Elizondo, Ray Chavez, and Zach Wallace

Prepared by  
Sandia National Laboratories  
Albuquerque, New Mexico 87185 and Livermore, California 94550

Sandia is a multiprogram laboratory operated by Sandia Corporation,  
a Lockheed Martin Company, for the United States Department of Energy's  
National Nuclear Security Administration under Contract DE-AC04-94AL85000.

Approved for public release; further dissemination unlimited.



Issued by Sandia National Laboratories, operated for the United States Department of Energy by Sandia Corporation.

**NOTICE:** This report was prepared as an account of work sponsored by an agency of the United States Government. Neither the United States Government, nor any agency thereof, nor any of their employees, nor any of their contractors, subcontractors, or their employees, make any warranty, express or implied, or assume any legal liability or responsibility for the accuracy, completeness, or usefulness of any information, apparatus, product, or process disclosed, or represent that its use would not infringe privately owned rights. Reference herein to any specific commercial product, process, or service by trade name, trademark, manufacturer, or otherwise, does not necessarily constitute or imply its endorsement, recommendation, or favoring by the United States Government, any agency thereof, or any of their contractors or subcontractors. The views and opinions expressed herein do not necessarily state or reflect those of the United States Government, any agency thereof, or any of their contractors.

Printed in the United States of America. This report has been reproduced directly from the best available copy.

Available to DOE and DOE contractors from  
U.S. Department of Energy  
Office of Scientific and Technical Information  
P.O. Box 62  
Oak Ridge, TN 37831

Telephone: (865) 576-8401  
Facsimile: (865) 576-5728  
E-Mail: [reports@adonis.osti.gov](mailto:reports@adonis.osti.gov)  
Online ordering: <http://www.osti.gov/bridge>

Available to the public from  
U.S. Department of Commerce  
National Technical Information Service  
5285 Port Royal Rd.  
Springfield, VA 22161

Telephone: (800) 553-6847  
Facsimile: (703) 605-6900  
E-Mail: [orders@ntis.fedworld.gov](mailto:orders@ntis.fedworld.gov)  
Online order: <http://www.ntis.gov/help/ordermethods.asp?loc=7-4-0#online>



## **Low Inductance Gas Switching**

**Chuck Harjes, Juan Elizondo, Ray Chavez, and Zach Wallace**

Sandia National Laboratories  
Advanced Accelerator Physics Department  
P.O. Box 5800  
Albuquerque NM 87185-1194

### **ABSTRACT**

The laser trigger switch (LTS) is a key component in ZR-type pulsed power systems. In ZR, the pulse rise time through the LTS is  $> 200$  ns and additional stages of pulse compression are required to achieve the desired  $< 100$  ns rise time. The inductance of the LTS ( $\sim 500$  nH) in large part determines the energy transfer time through the switch and there is much to be gained in improving system performance and reducing system costs by reducing this inductance. The current path through the cascade section of the ZR LTS is at a diameter of  $\sim 6$ " which is certainly not optimal from an inductance point of view. The LTS connects components of much greater diameter (typically 4'-5'). In this LDRD the viability of switch concepts in which the diameter of cascade section is greatly increased have been investigated. The key technical question to be answered was, will the desired multi-channel behavior be maintained in a cascade section of larger diameter.

This LDRD proceeded in 2 distinct phases. The original plan for the LDRD was to develop a promising switch concept and then design, build, and test a moderate scale switch which would demonstrate the key features of the concept. In phase I, a switch concept which meet all electrical design criteria and had a calculated inductance of 150 nH was developed. A 1.5 MV test switch was designed and fabrication was initiated. The LDRD was then redirected due to budgetary concerns. The fabrication of the switch was halted and the focus of the LDRD was shifted to small scale experiments designed to answer the key technical question concerning multi-channel behavior.

In phase II, the Multi-channel switch test bed (MCST) was designed and constructed. The purpose of MCST was to provide a versatile, fast turn around facility for the study the multi-channel electrical breakdown behavior of a ZR type cascade switch gap in a parameter space near that of a ZR LTS. Parameter scans on source impedance, gap tilt, gap spacing and electrode diameter were conducted.

(left blank intentionally)

(left blank intentionally)



## CONTENTS

I. Introduction.....	8
II. Phase I – 1.5 MV switch Design.....	11
III. Phase II – Phase II – Small Scale Switch Test Bed.....	21
IV. Result from MCST Experiments.....	31
V. Summary.....	40
VI. References.....	41

## FIGURES

1. Basic circuit of a typical pulsed power system like ZR.....	8
2. Cross-sections of the ZR laser triggered switch . . . . .	9
3. Open shutter photograph of an operating ZR LTS showing multi-channel breakdown behavior in the cascade section.....	10
4 Electric field plot of an early version of the ZR.....	12
5 LTS concept extrapolated from existing design in which the cascade electrode diameters have been moved to near PFL/IS diameters to minimize inductance. This is likely not a practical switch design.....	12
6 Electric field plot of an LTS concept with no oil envelope, a hybrid trigger section and large diameter cascade electrodes. Marx (1) - 32 ea., 700 nF, 100 kV capacitors, 110 kJ max. energy.....	14
7 The MUTTS facility at the University of Missouri would allow testing in the 1.5-2.5 MV range. It is basically a module of ProtoII Intermediate Store (2) - 2 parallel 7nF water caps., 60 kJ max. energy.....	16
8 Design drawing depicting how the 1.5 MV LDRD switch would have been mounted in the MUTTs test bed.....	16
9 Results of an electrostatic field simulation of the final switch design.....	17
10 Plot of the electric field in the 10 cascade gaps.....	17

11	Assembly drawing of the final 1.5 MV switch design.....	18
12.	Block diagram of the multi-channel switch test bed (MCST).....	21
13	Over-head Photo of the assembled MCST system.....	22
14	Photo of the MCST Marx bank.....	23
15	Photos of the MCST test chamber with lid removed from above and through a view port.....	24
16	Circuit diagram of MCST has configured in initial tests. ....	26
17	Photo of a 2 channel breakdown (double) from an early shot on MCST.....	27
18	Photo taken through the MCST tank front port showing the PG installation.....	27
19	Typical MCST load voltage waveforms before and after PG installation.....	28
20	Typical load voltage waveform with a 15 kΩ shunt resistor across the PG.....	28
21	Cross-section drawing and photo of the water capacitor test assembly.....	29
22	Circuit diagram of MCST with reconfigured test assembly including a water capacitor (IS) and a trigger gap.....	30
23	Load voltage and current waveforms from MCST shot # 640 which was a 5 channel breakdown shot .....	30
24	Photo of the 5 channel breakdown on MCST shot 640.....	30
25	Photos of experimental setups where inductance was added to increase circuit impedance. The top photo shows the 8 x straps setup and the bottom photo shows the 8 x L1 setup shot.....	33
26	Drawing and spreadsheet showing how inductances for the various setups was estimated.....	34
27.	Data and plot showing how the average # of channels declines as circuit impedance increases.....	35

28. Photo, data, and plot from the gap tilt experiments.....	36
29. Photos of the setups with 1.5”, 5.5”, and 11.5” diameter electrodes.....	37
30. Data and plot from electrode diameter experiments showing how the average # of channels increases significantly as electrode diameter increases.....	38
31. Data and plot from preliminary gap separation experiments showing how the average # of channels varies with gap spacing. More data and analysis is required to draw conclusions from these experiments.....	39

## TABLES

1. ZR single module parameters.....	11
2. Summary of the electrical study of lower inductance switch concepts conducted during the 1 <sup>st</sup> 6 months of the LDRD.....	13
3. Summary of the mechanical design effort and key technical issues .....	19
4. Cost estimate for switch hardware .....	20
5. Nominal parameters for a ZR LTS compared with the range available on MCST.....	21
6. Summary of experiments conducted on MCST.....	26

## INTRODUCTION

In ZR[1] type pulsed power systems, the laser triggered gas switch (LTS) is typically positioned between the intermediate store (IS) and the pulse forming line (PFL) as shown in Fig. 1. These lines are normally coaxial with inner conductors several feet in diameter (4-5). When closed the LTS electrically connects the inner conductors of the IS and PFL. The inductance of the switch in large part determines what the energy transfer time from the IS to the PFL will be. In ZR, the transfer time is  $> 200$  ns and additional stages of pulse compression are required to achieve pulse rise-times under 100 ns. If the LTS inductance could be reduced significantly, it might be possible to eliminate a stage of pulse compression and make a ZR like system simpler and reduce cost. The primary purpose of this LDRD is to investigate methods for reducing the inductance of an LTS.

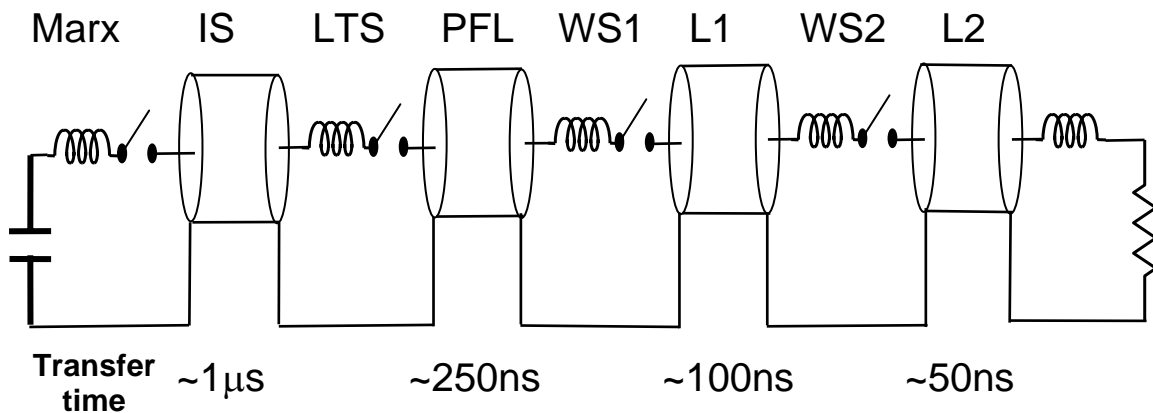


Figure 1. Basic circuit of a typical pulsed power system like ZR.

The ZR LTS is shown in Fig. 2. It consists of a trigger section which is closed by a single on axis arc and a cascade section which is closed by multiple arcs. The cascade section is about 25" long and the electrodes have a diameter of  $\sim 6.5$ ". The total switch inductance is  $\sim 500$  nH and the cascade section accounts for  $\sim 63\%$  of the total. In Fig. 3, an open shutter photograph of an operating LTS is shown. The multi-channeling behavior in the cascade section is a key feature in good switch performance. The inductance of a coax scales as  $L_n$  (outer diameter/inner diameter). With multi-channel behavior the effective inner diameter (ID) of the cascade section is near that of the electrodes. If it were to operate in a single channel mode, the effective ID would be considerably less and the inductance would be much higher. In this LDRD the viability of switch configurations in which the diameter of cascade section is greatly increased perhaps to diameters comparable to that of the IS and PFL inner conductors have been investigated. The key technical question to be answered was, will multi-channel operation be maintained in a cascade section with larger diameter.

The LDRD has proceeded in 2 distinct phases. The original plan for the LDRD was to design, build, and test a moderate scale switch. In phase I, a 1.5 MV switch was designed and fabrication was initiated. A test plan was developed and an agreement with the University of Missouri to test the switch in the MUTT's test bed was in place. The LDRD was then redirected due to budgetary concerns. The fabrication of the switch was

halted and the focus of the LDRD was shifted to answering the key technical question in a smaller scale experiment. In phase II, a small test bed was designed, built, and testing on a simple 2 electrode gap was performed at SNL. Below both phase I and II are described in detail. The results of phase II experiments are then presented followed by a summary.

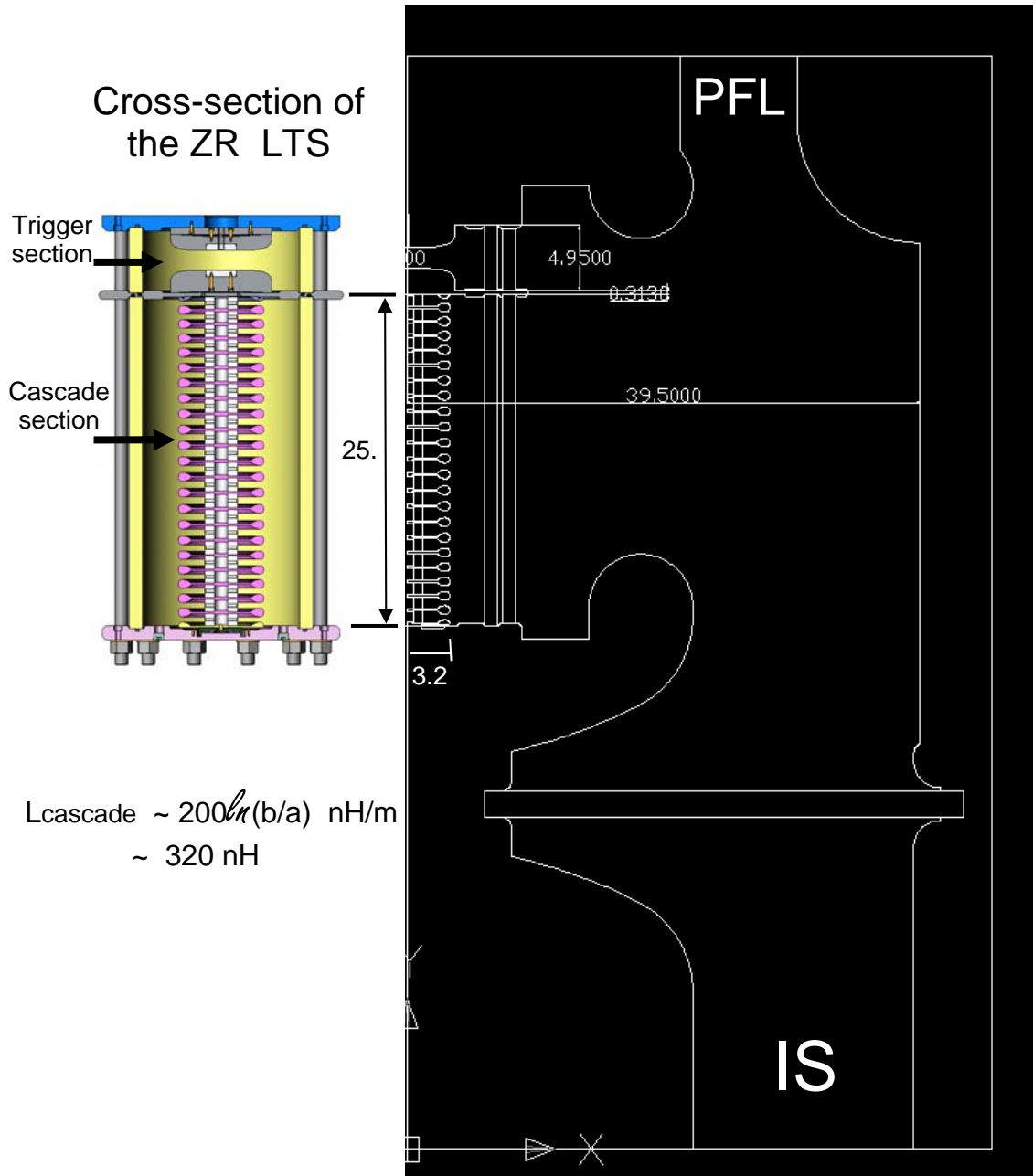


Figure 2. Cross-sections of the ZR laser triggered switch .

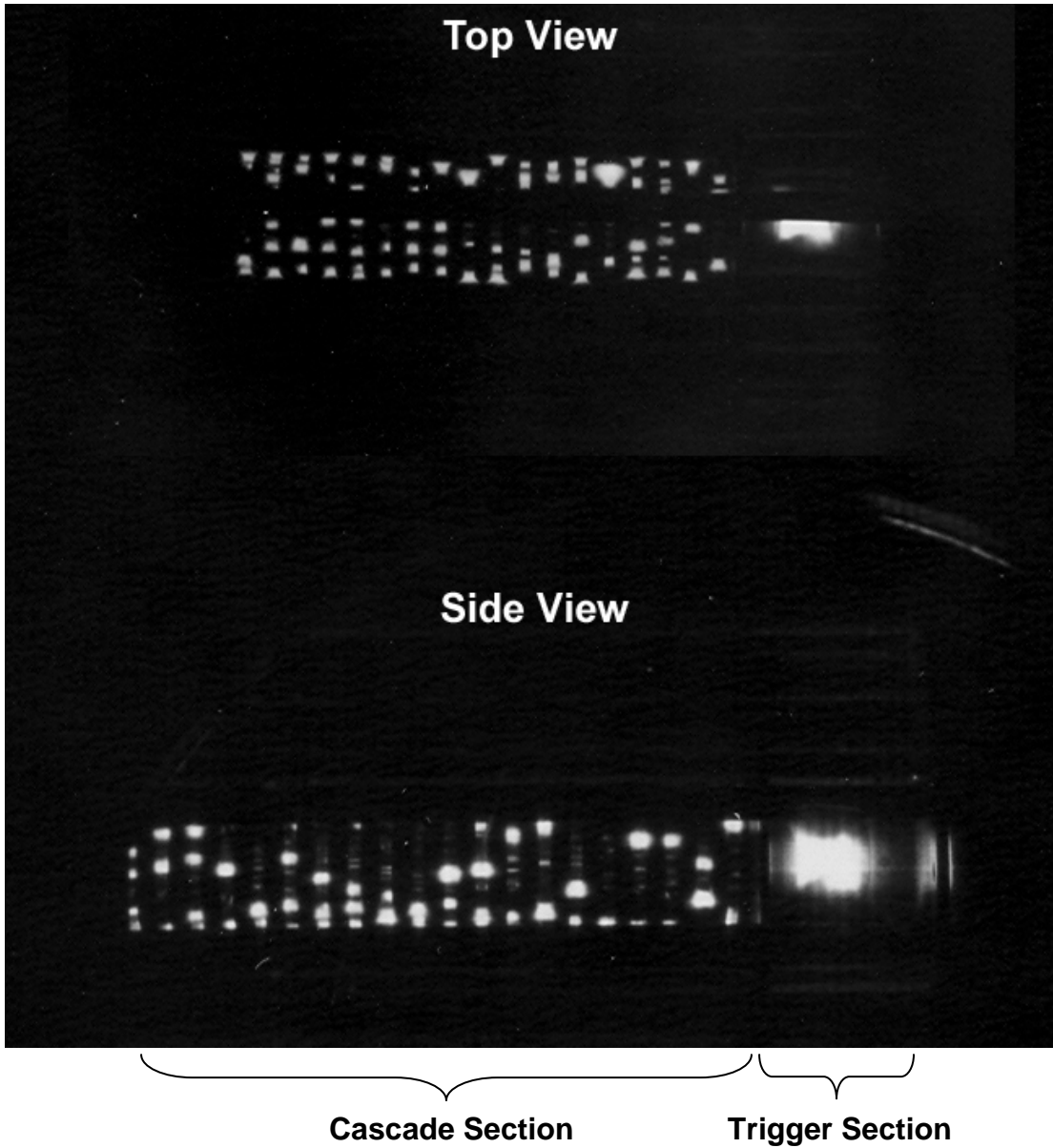


Figure 3. Open shutter photograph of an operating ZR LTS showing multi-channel breakdown behavior in the cascade section.

## II. Phase I – 1.5 MV Switch Design

ZR consists of 36 pulsed power modules which are essentially connected in parallel to drive the ZR load. Some parameters for a single ZR pulsed power module are listed in table 1. The LTS is the key switch in the system because it is externally triggered and is used to synchronize all 36 modules. The ability to externally adjust the switch pressure and/or the command trigger time gives this switch a relatively wide operational range. In addition, the closed switch circuit parameters (resistance and inductance) are relatively consistent over its operational range. The water switches (WS), on the other hand, are self-breaking and have several negative aspects. They introduce significant timing jitter which scales inversely with applied  $dV/dt$  (ie. the more pulse compression the switch does the greater the jitter will be)[2]. The water switches can also be relatively lossy. The electrical bottleneck in a ZR module is the 1<sup>st</sup> water switch because its closed resistance increases as its gap is increased. When the module's input voltage/power is increased, the WS gap must be opened for operation at a higher voltage/power. The increased switch losses, however, decreases the module's efficiency and at some point an increase in input power does not result in increased output power. In addition, the mechanical shock wave generated by water switch closure is an operational nuisance due to the collateral damage it causes. This also worsens as the switch does more pulse compression. For these reasons, there is much to be gained by reducing the work the WSs have to do or perhaps eliminating a stage completely.

Marx		IS		LTS		PFL		WS1		L1		WS2	
Ns =	60	Z=	3.82 $\Omega$	L=	500 nH	Z=	2.7 $\Omega$	L*=	60 nH	Z=	4.2 $\Omega$	L*=	7 nH
Vch =	85 kV	T=	90 ns	R=	0.1 $\Omega$	T=	42 ns	R*=	0.35 $\Omega$	T=	32 ns	R*=	0.35 $\Omega$
Cout =	43.3 nF	C=	23 nF			C=	15.6 nF			C=	7.6 nF		
R =	1.4 $\Omega$												
L =	13 $\mu$ H												

Table 1. ZR single module parameters.

An electric field strength plot from a simulation on an early version of the ZR LTS is shown in Fig. 4. This switch design has been developed over a number of years and has been extensively tested. In the design, components are sized to ensure that field strengths remain within established limits and that the fields in the cascade gaps are approximately uniform from one end of the cascade section to the other. Assuming multi-channel behavior, the calculated inductance of the cascade section of the switch in Fig. 4 is 390 nH (the total switch inductance is  $\sim$  500 nH). The current path through the switch is at a diameter of  $\sim$  6" which is certainly not optimal from an inductance point of view. As an exercise, the inductance of the switch concept of Fig. 5 where the current path through the switch is at about the same diameter as the IS and PFL inner conductors was calculated. In this switch, the oil envelope around the switch has been eliminated and a hybrid trigger section utilized [3]. Assuming multi-channel behavior, the calculated inductance of this switch is 127 nH which is nearing that of WS1, 60 nH. If the inductance of the LTS could be reduced to this level, the performance of a ZR like system would certainly be enhanced.

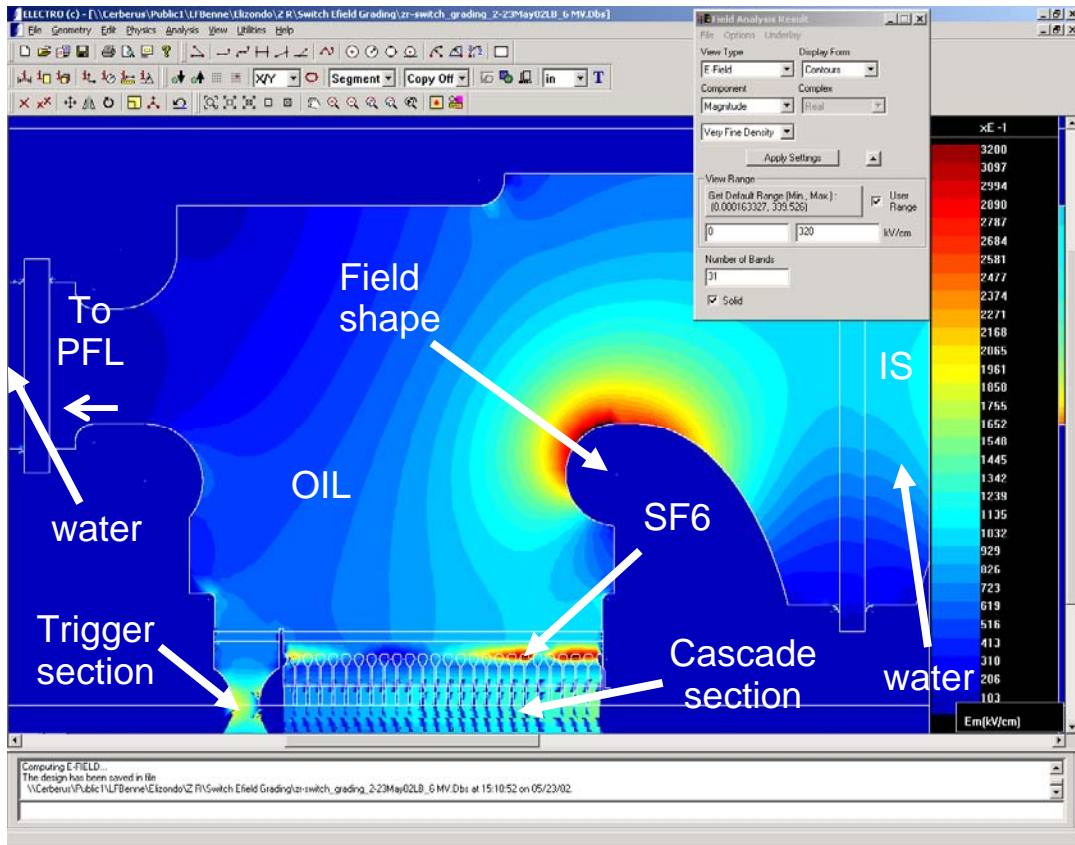


Figure 4. Electric field plot of an early version of the ZR.

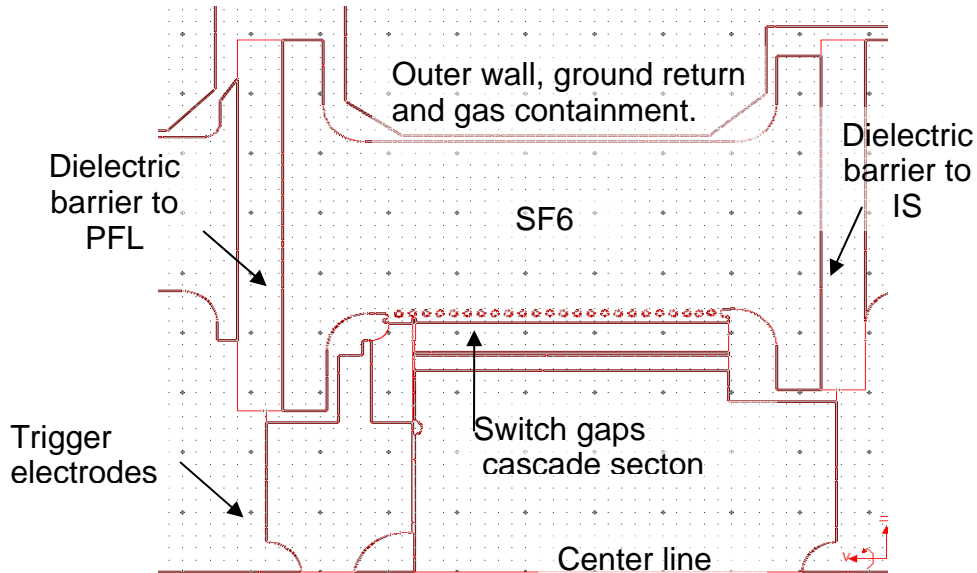


Figure 5. LTS concept extrapolated from existing design in which the cascade electrode diameters have been moved to near PFL/IS diameters to minimize inductance. This is likely not a practical switch design.

The concept of Fig. 5 demonstrates that there is potential for significant switch inductance improvement, but, it is not a practical switch design. In a practical switch, there are many technical issues to be addressed which are briefly summarized in the following;

- 1) The electric fields in the switch must be carefully controlled. Peak electric field strengths must be kept below established limits in many locations.
- 2) The electric field distribution in the cascade gaps must be nearly uniform from one end of the switch to the other.
- 3) The switch must also be mechanically sound. With the elimination of the oil envelope around the switch, the mechanical design will be a significant deviation proven designs. The IS and PFL barriers have to support the 30-60 psi SF6 pressure in the switch volume.

In the 1<sup>st</sup> 6 months of this LDRD, a number of concepts were studied primarily from an electrical perspective to come up with a practical concept that had the potential of operating at significantly lower inductance. The results of this study are summarized in Table 2.

The LDRD accomplishments for the 1st half year are summarized here: Several alternative configurations have been investigated. In all cases the plastic envelop enclosing the switch gas in present LTSs has been eliminate. The switch envelope in the alternative configurations is the outer conductor of the system (metal). There is no oil or water around the switch.

- 1 - Successfully developed several options for the electrode/cascade region that can be used in a metal envelop gas switch. The goal was to uniformly distribute the electric field across all the cascade gaps.
  - Variable gap spacings with the same diameter electrodes throughout the cascade section. This configuration requires the outer metal shell be tapered somewhat, but, offers the lowest inductance.
  - Consistent gap spacings throughout the cascade section with variable electrode diameters. This option allows a non-tapered outer ground shell, but, the inductance is not as low as possible.
  - Variable gap spacings and variable electrode diameters with a non-tapered outer ground shell.
  - Incorporated the Hybrid-trigger section to eliminate trigger inductance penalty.
- 2 - Eliminated the need for the I-Store field shaper which further reduces system size.
- 3 - I-Store termination has been simplified and tapered to improve fields and the switch transition.
- 4 - Developed a preliminary mechanical model for the switch envelop utilizing a solid center to reduce gas load penalty and enhance safety.

Table 2. Summary of the electrical study of lower inductance switch concepts conducted during the 1<sup>st</sup> 6 months of the LDRD.

In Fig.6, the result of an electrostatic simulation on the most promising switch concept studied is shown. In this concept the oil envelope is eliminated and a hybrid

trigger section is used. The cascade electrodes are pushed to larger diameters and the diameters are varied along the length of the switch as shown. In addition the electrode gap spacings are allowed to vary. In this way, uniform field grading in the cascade gaps was achieved without having to include a large field shaper. The calculated inductance of this switch concept, **assuming multi-channel behavior**, was 150 nH. In a brief assessment of the mechanical issues with this concept, they were deemed somewhat challenging, but, none were considered unmanageable. With this, the study of new switch concepts was de-emphasized and the focus of the project was shifted to designing a switch to test. Since the test switch needed to be affordable within the LDRD budget, a full scale 6 MV ZR type switch could not be considered. Consequently, the decision was made to proceed with the design of a moderate scale switch which could demonstrate the key and unique electrical/mechanical features of the concept shown in Fig. 6.

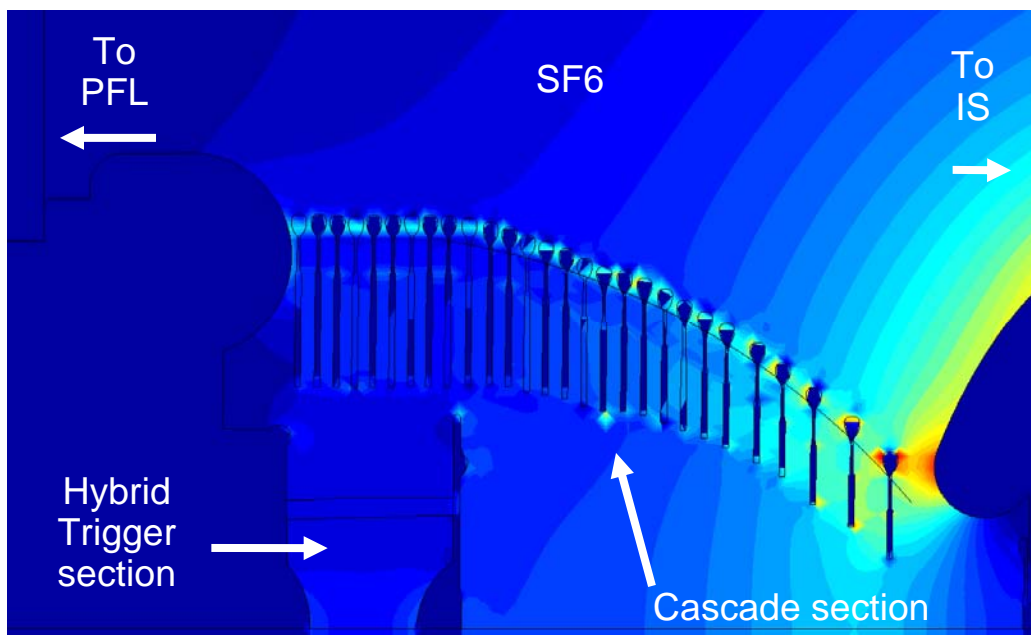


Figure 6. Electric field plot of an LTS concept with no oil envelope, a hybrid trigger section and large diameter cascade electrodes.

The switch that was designed for testing in this LDRD was the product of a full blown design effort involving departments 1644 (electrical), 1639 (mechanical), and 1637 (drafting). The design effort started in the 2<sup>nd</sup> half of the 1<sup>st</sup> year of the LDRD and was completed early in the 2<sup>nd</sup> year. An agreement was negotiated early in the process with the University of Missouri to test the switch in an existing test bed called MUTTs [4] which is described in Fig. 7. Consequently, the switch was designed to mate with and fit within the constraints of the test bed as shown in Fig 8. The switch was designed to operate at 1.5 MV, included 10 cascade gaps ranging in diameter from 8” to 17”, and used a conventional trigger section. A calculated electrostatic field plot of the switch is shown in Fig. 9 and a graph of the acceptably uniform electric field distribution in the cascade gaps is shown in Fig. 10. The primary objectives of the planned tests were to;

- 1) demonstrate the mechanical soundness of a switch design without an oil envelope and flat barriers to contain the 32 psi switch pressure,
- 2) demonstrate the successful operation of the unique cascade section design with variable electrode diameters and gaps, and
- 3) determine if multi-channel behavior will occur between electrodes of significantly larger diameters. If there is a strong diameter dependence in multi-channel behavior, the range of diameters in the switch should clearly show it.

In the design effort, the details of manufacture, assembly, and operation were thoroughly examined and the necessary tradeoffs were negotiated. An assembly drawing of the final design is shown in Fig. 11 and a summary of the mechanical design effort and associated key issues is given in Table 3 [5]. A complete drawing package for the switch and supporting hardware was finished and has been archived in <\\Cerberus\Public\Harjes\UM switch files>. These files include;

- Universal E-drawing File
- Solidworks Models and Drawings
- PDF's of the Solidworks drawings
- 2D and 3D files for electrical analysis
- Various pictures and illustrations

Some of the long lead materials for the switch were ordered near the end of the 1<sup>st</sup> year of the LDRD and the procurement process for hardware began in earnest after the drawings were finished early in the 2<sup>nd</sup> year. When the hardware cost estimates shown in Table 4 came in, the LDRD project was **re-directed by management** due to budgetary concerns. The test switch was going to use about half of the LDRD's FY budget and this was deemed unwise. The procurement of hardware was halted and the planned moderate scale experiments on the 1.5 MV switch were cancelled.

After going through the mechanical design effort, confidence was high that the switch would be mechanically sound. Confidence was also reasonably high (as high as it could be without testing) that the switch would operate electrically at the 1.5 MV level. The question concerning multi-channel behavior in the cascade section remained as the key technical issue. Consequently, the project was directed to plan smaller scale (1 or 2 gap) experiments which would be directed toward characterizing multi-channel behavior in cascade type gaps as a function of a few parameters to include electrode diameter.

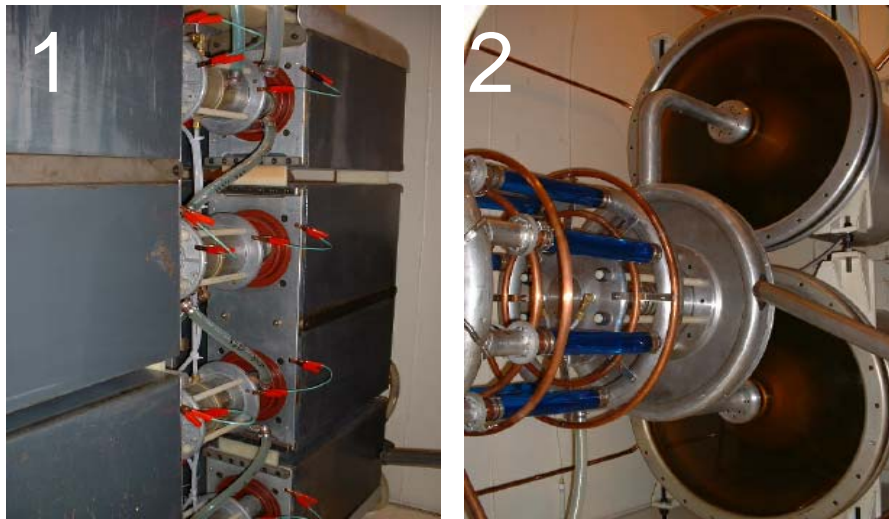


Figure 7. The MUTTS facility at the University of Missouri would allow testing in the 1.5-2.5 MV range. It is basically a module of ProtoII;  
 Marx (1) - 32 ea., 700 nF, 100 kV capacitors, 110 kJ max. energy  
 Intermediate Store (2) - 2 parallel 7 nF water capacitors, 60 kJ max. energy

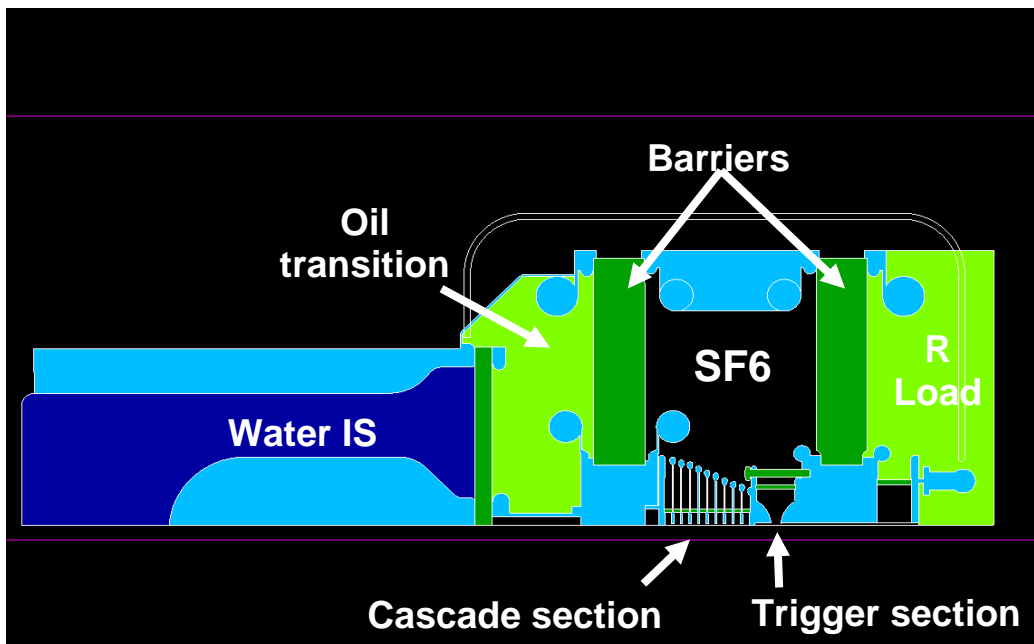


Figure 8. Design drawing depicting how the 1.5 MV LDRD switch would have been mounted in the MUTTS test bed.

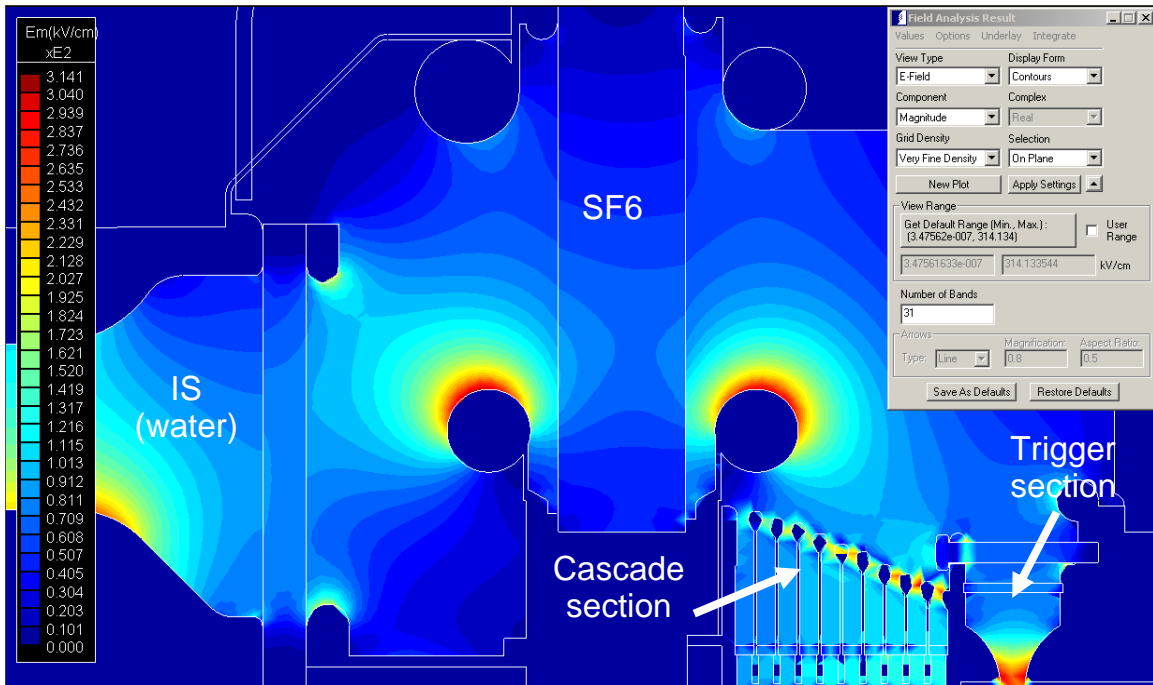


Figure 9. Results of an electrostatic field simulation of the final switch design.

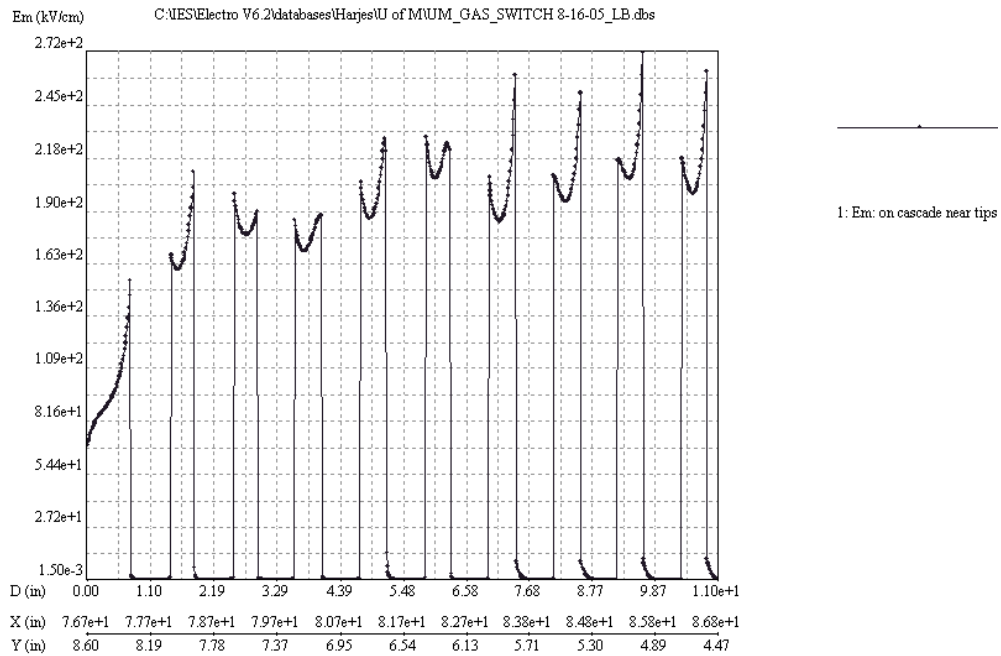


Figure 10. Plot of the electric field in the 10 cascade gaps.

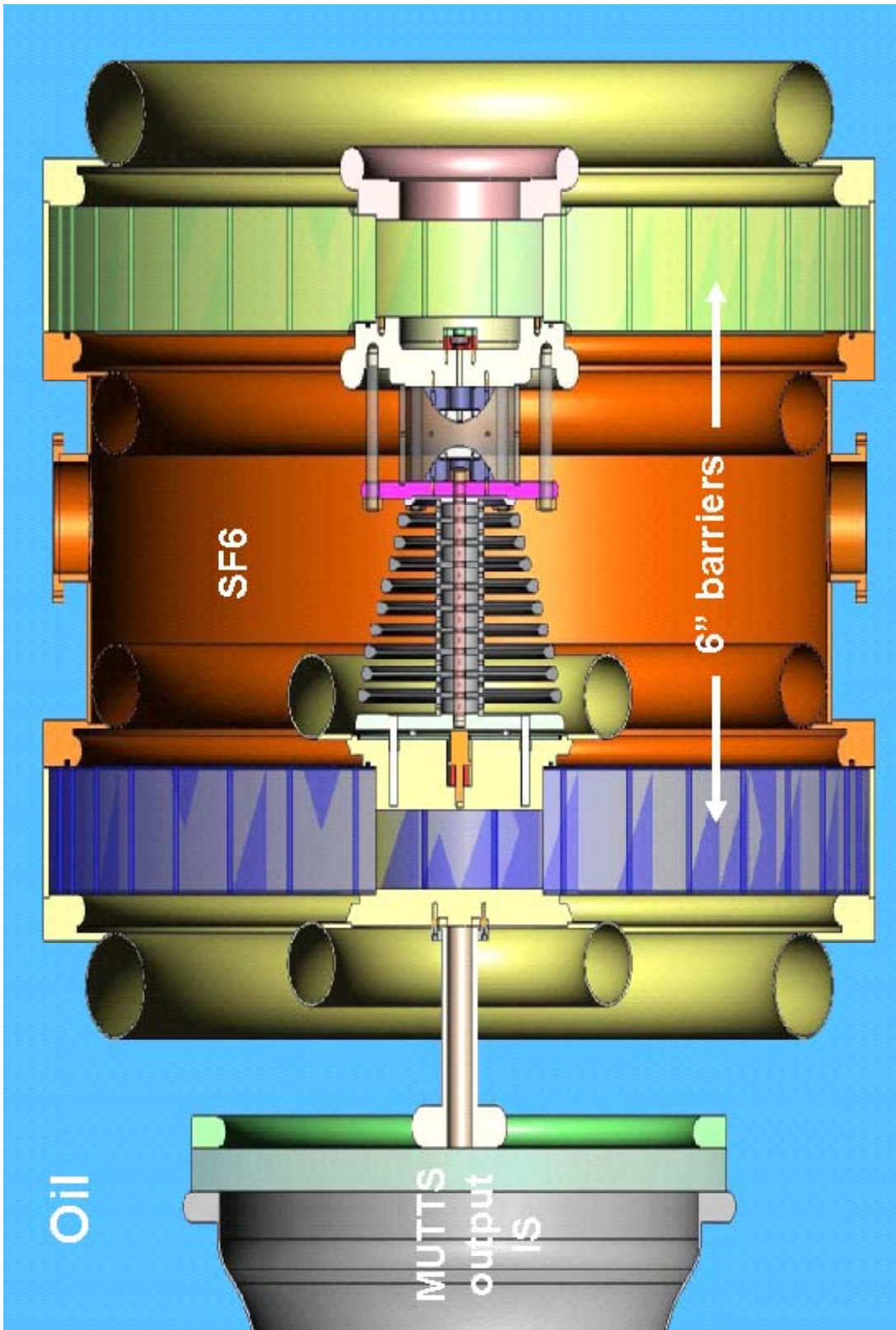


Figure 11. Assembly drawing of the final 1.5 MV switch design.

### **Mechanical Design Effort Summary**

SolidWorks CAD software was used to model the switch and examine design issues. CosmosWorks finite element analysis software was used to perform static elastic analysis of the barriers and major pressure-containing stainless steel components. Design iterations were based on electrical analyses of conductor profiles and geometry of modeled components. Manufacturing methods were considered along with dimensional tolerance requirements in designing the large flanges and polyurethane barriers.

### **Key Mechanical Issues**

#### **Barrier Stress**

The large flat barriers required for this design exhibit relatively large stress levels and deflections when exposed to moderate stress pressures. An operating pressure of 35psi was used for the design of the switch. A factor of safety of 5 based on the ultimate strength of the polyurethane limited acceptable stress to 1,100psi in the barriers. Static elastic finite element analysis of the barriers showed that a 6 inch barrier thickness was sufficient to keep stresses below the acceptable level through the bulk of the barrier. Higher localized stresses near interfaces with the stainless steel switch were present. These were caused by the relative stiffness of the steel flanges and affected only negligible regions in the barrier surfaces.

#### **Barrier Deflection**

A modulus elasticity of 80,000psi was used in the finite element analysis of the barriers. This is the lower value of the acceptable range, (80,000psi to 140,000psi) dictated by *Material Specification, High Durometer Polyurethane* (SS-T90184 Material Specification 120604). The lower value was chosen to conservatively predict the deflection. Finite element analyses showed that the relative deflection of the barriers, when subjected to a 35psi internal pressure, could be as high as 1.2 inches. This became a critical design parameter as the internal components of the switch had to accommodate the deflection.

#### **Switch Support**

The internal components of the switch are structurally supported by the barriers. The switch design must accommodate barrier deflection under internal pressure. In order to accomplish this, the cascade and gap sections of the switch incorporate a spring-loaded linearly expandable connection. This allows the internal switch components to move relative to the central flange as the flange follows barrier deflection. To maintain the electrical profile of the switch geometry an internal, electrically insulating rod is used to clamp the spacers and plates of the cascade section. The motion of the barriers relative to the central switch components is confined to a section electrically protected by the internal field shaper.

#### **Flange Design**

Thick sections were required to allow field-shaping profiles to be machined into the flanges. The internal flanges were designed to accommodate the spring-loaded slip connection. Threaded holes in one internal flange allow for attachment of insulating rods used to locate and hold the gap assembly together. The outer flanges incorporate external walls used to locate and add support to the barriers. O-ring groves are included in the flanges to allow sealing of the internal pressure.

Table 3. Summary of the mechanical design effort and key technical issues[5].

**Cost Estimate For LDRD UM Switch      11/16/05**

Barriers	\$44,000.00
Conductor, Outer	\$25,000.00 (2 forging supplied)
Clamp Barrier Lower	\$10,000.00 (1 forging supplied)
Clamp Barrier Upper	\$8,500.00 (1 forging supplied)
Lower Center Plate wo/Field Shaper	\$3,500.00
Lower Center Plate w/Field Shaper	\$6,000.00
Spacers (10 ea.)	\$2,000.00
Electrode Disks	\$19,000.00
Center Rod	\$1,000.00
Trigger Section	\$12,000.00
Upper Barrier Center Plate	\$5,500.00 (center w/solid Field Shaper)
Upper Barrier Center Plate	\$4,000.00
	<b>Total: \$140,500.00</b>

Note: The four flanges purchased are included as supplied materials.  
 Barrier quote from Globe Composites uses existing tooling – delivery 1/10/05  
 Delivery of all items by 1/15/05 or sooner  
 Pricing does not include optics  
 Pressure test at SNL ~ \$4,000.00  
 Assembly at SNL for testing - ~\$2,000.00  
 Shipping to University of Missouri Rolla - ~\$1,500.00

Table 4. Cost estimate for switch hardware [5].

### III. Phase II – Small Scale Switch Test Bed

The purpose of the small scale switch test bed was to provide a versatile, fast turn around facility for the study the multi-channel electrical breakdown behavior of ZR type cascade switch gap in a parameter space near that of a ZR LTS. Gaining a better understanding and perhaps characterizing of how key parameters (especially electrode diameter) effect multi-channel behavior was of greatest interest. In table 5, the parameters that were considered in the design of the test bed are compared to those of a ZR LTS (MCST only comes up short on 2 parameters, current and # of gaps). The Multi-channel switch test bed (MCST) is depicted in Fig.12. The starting point for the design of MCST was an existing system, the Insulation Tester locate in building 961, which seemed capable of providing a reasonable drive for the required tests. With the existing oil tank, Marx bank, and control/DAS system already in place, all that needed to be designed/fabricated was the test chamber (with associated support and lifting hardware), the test switch, the connections to the existing system, and the diagnostics for the test gap. The photographs in Figs. 13–15 show some of the key components of the system.

parameter	ZR - LTS	MCST
voltage	~ 250 kV	100 - 600 kV
current	~ 650 kA	0 - 100 kA
gap	0.34"	0 - 2"
pressure	32 psi	0 - 32 psi
electrode dia.	6.5"	0 - 24 "
Voltage Trise	~ 6 ns	6 - 200 ns
# gaps	25	1 - 2
gas	SF6	any non-haz.

Table 5. Nominal parameters for a ZR LTS compared with the range available on MCST.

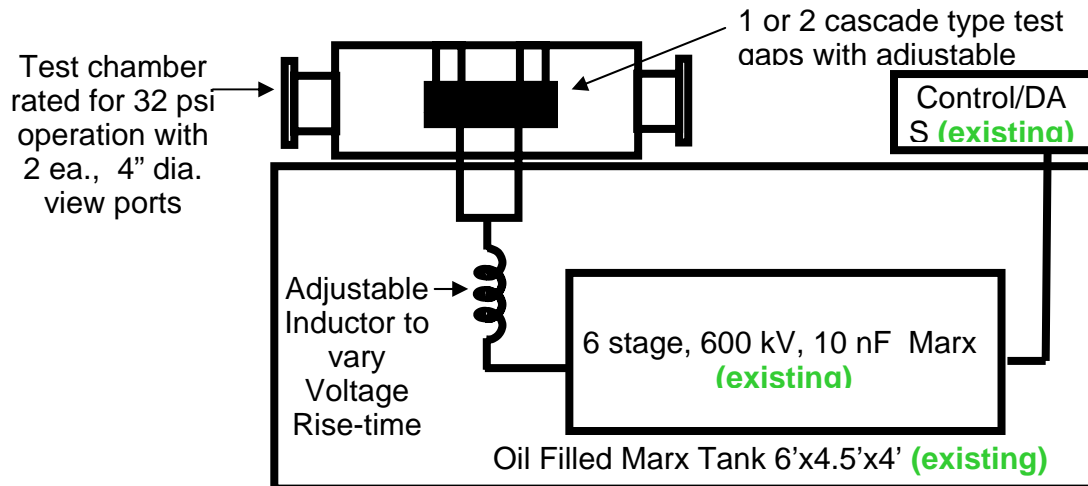


Figure 12. Block diagram of the multi-channel switch test bed (MCST).

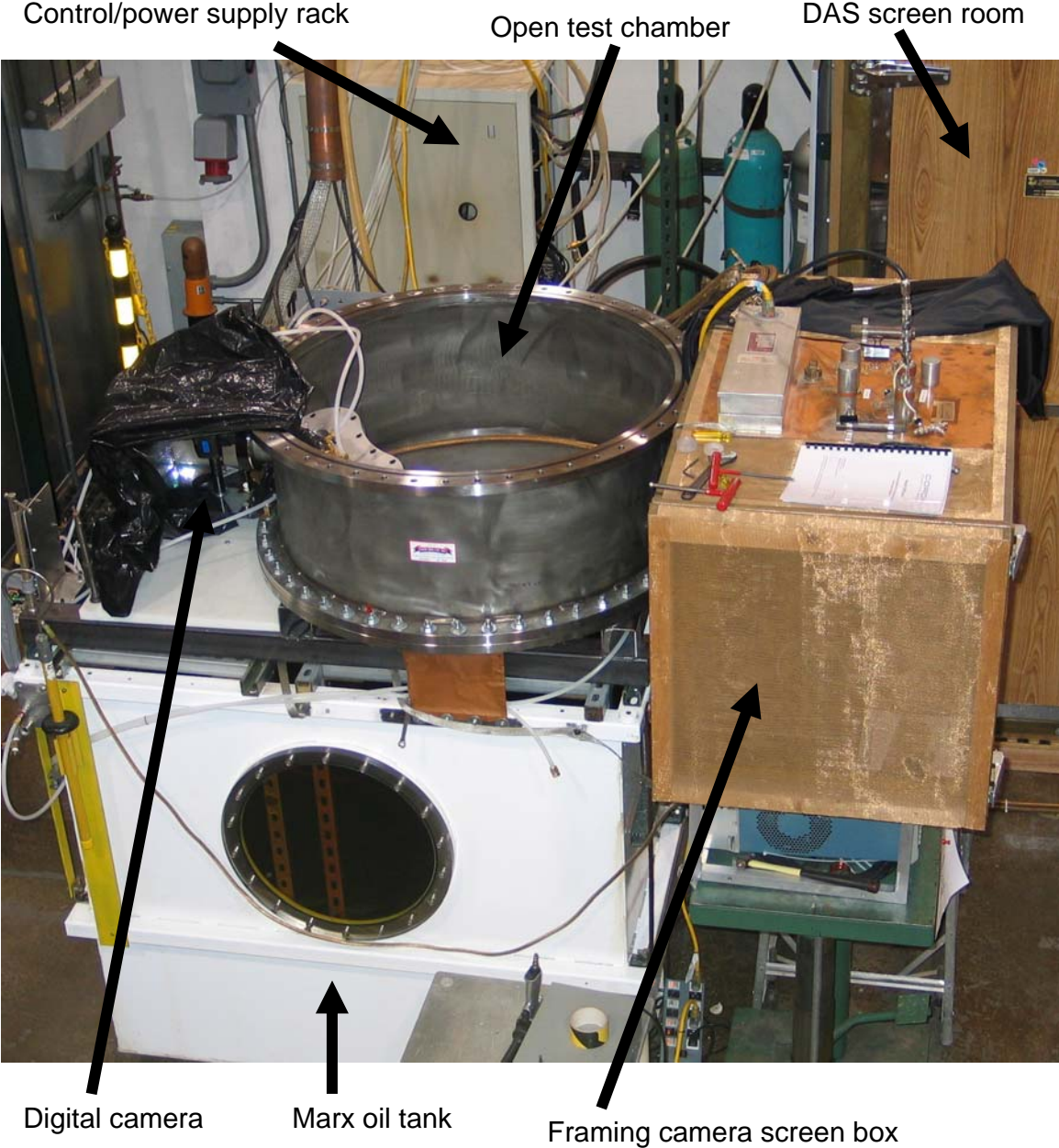


Figure 13. Over-head Photo of the assembled MCST system.

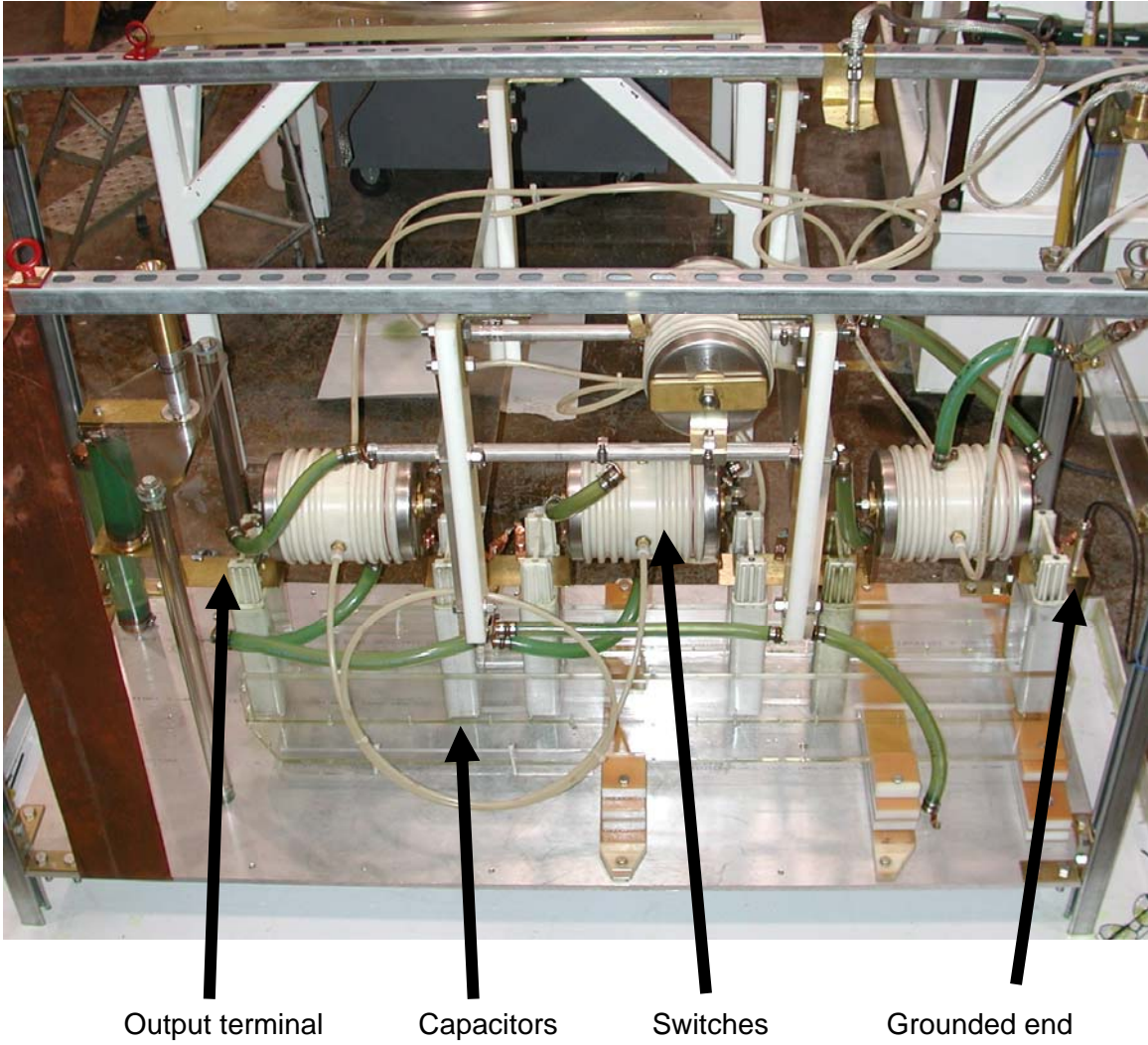
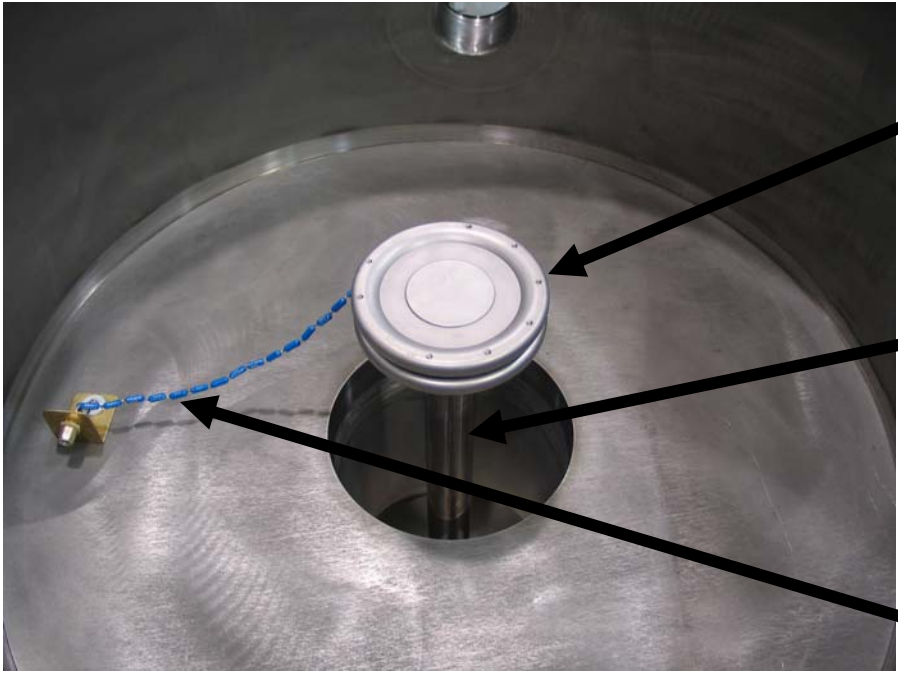


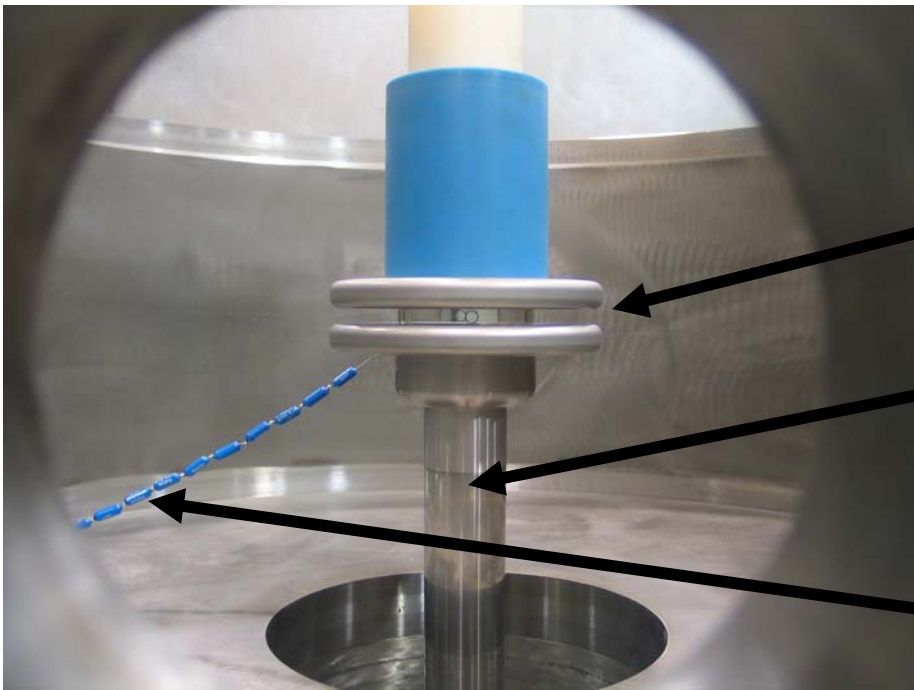
Figure 14. Photo of the MCST Marx bank.



Test gap  
with 6.5" dia.  
electrodes

HV  
input  
stalk

Load  
voltage  
monitor



Test gap  
with 6.5" dia.  
electrodes

HV  
input  
stalk

Load  
voltage  
monitor

Figure 15. Photos of the MCST test chamber with lid removed from above and through a view port.

The primary diagnostics used in all tests were; a 15 k $\Omega$  resistive voltage monitor connected to the high voltage test electrode for monitoring load voltage, a collection of 4 parallel, 0.1 $\Omega$  CVRs (located 90° apart) connecting the top test electrode to ground for monitoring load current, a digital open shutter camera for recording the image of the breakdown, and on some shots, a framing camera was used as well.

A summary of the MCST shot log is given in Table 6 and the basic circuit for MCST is shown in Fig. 16. Once the system had been assembled and checked out to demonstrate proper functionality, the 1<sup>st</sup> objective was to achieve consistent multi-channel behavior. The initial tests were in 1 atm. air on a pair of 6.5” diameter cascade electrodes (from an existing ZR LTS) set to the nominal (0.34”) gap. A typical photo of a 2 channel (double) breakdown obtained in an early shot series is shown in Fig. 17. Under these conditions, ~ 50% of the shots were singles, ~ 50% were doubles, and there was an occasional triple. When the series was repeated in 1 atm. SF<sub>6</sub>, ~80% of the shots were singles.

After a brief scan of easily adjustable parameters with no progress, a system modification was done to increase the dV/dt of the voltage pulse applied to the test gap. A self-breaking peaking gap (PG), shown in Fig. 18, was added between the output of the Marx and input to the test chamber. The PG was set to hold off until the Marx output voltage was nearing peak (a few 100 ns). Load voltage waveforms from before and after PG installation are compared in Fig. 19. The load voltage rise-time to break with the PG is ~ 6 ns. According to electro-dynamic simulations of an LTS done by Rosenthal [6], this is about what a cascade gap in an operating LTS would see. However, even with this refinement to the system, the statistics were essentially unchanged (~ 80% of the shots were still singles).

In an operating LTS, the voltage applied to the switch rises slowly as the IS is charged by the Marx ( duration ~1  $\mu$ s). This voltage is distributed across the cascade and trigger gaps. When the trigger gap closes, the voltage in the switch is rapidly redistributed. The voltage on an individual cascade gap then rises from the slow ramp level to breakdown in ~ 6ns. This type of applied voltage waveform is not well mimicked by the waveforms of Fig. 19, but, by simply connecting a shunt resistor (~15 k $\Omega$ ) in parallel with the PG, the load voltage waveform shown in Fig. 20 was obtained. With this refinement, however, the statistics were again essentially unchanged (~80 % singles). The shunt resistor value was also varied to modify the amplitude of the slow ramp relative to breakdown voltage with no effect on the statistics.

This lead to the conclusion that the problem must be associated with current. More prompt current needed to be made available to the test gap in order to support the desired multi-channel behavior (ie. the impedance of the source needed to be lower). To do this, new hardware was designed and fabricated and the test setup was modified as follows;

- 1) the PG in the oil tank was removed and replaced with a short low inductance connection between the Marx and the input to the test chamber.
- 2) A small (~0.8 nF) water capacitor was added in the test chamber connected between the HV input stalk and ground. This capacitor would be like an IS , slowly charged by the Marx, but, able to rapidly provide current to the test gap.

- 3) A self-breaking trigger gap (TG) was added in the test chamber between the top of the HV input stalk and the bottom test gap electrode.

A drawing of the new test setup along with a photo is shown in Fig. 21. The new circuit configuration is represented in Fig. 22 and the resulting load voltage and current waveforms are shown in Fig. 23. With this modification, **consistent multi-channel behavior was finally achieved**. A photograph of a 5 channel breakdown in 32 psi SF6 between 6.5" diameter electrodes with nominal gap is shown in Fig. 24. Under these conditions, multiple channels were observed in >90% of the shots and on average 2.8 channels were observed per shot. The system was now ready for parameter studies to characterize multi-channel behavior.

shot #s	dates	description of tests	result
1 - 116	12/4/06 - 2/19/07	system checkout	
117 - 137	2/20/2007	ring-over shots	
138 - 157	3/9/2007	air, 1 atm, 6.5" elect., 0.34" gap	55% singles
158 - 179	3/9/2007	SF6, 1atm, 6.5" elect., 0.34" gap	80% singles
178 - 197	3/12/2007	SF6, 30psi, 6.5" elect., 0.34" gap	90% singles
198 - 227	3/13/2007	bead blasted, SF6, 30psi, 0.34" gap	85% singles
229 - 280	3/20/07 - 3/22	PG installed, scan PG pressure	80-90 % singles
280 - 313	3/23 - 5/30	added R across PG	80-90 % singles
314 - 421	4/18 - 5/30	new operator, set-up, practice	
422 - 624	6/20/07 - 7/25/07	opposing knife edge electrodes, various widths/gaps	mostly singles
625 - 634	8/10/07 - 8/13/07	<b>new set up w/IS</b> , SF6, 14psi, 6.5" elect., 0.34" gap, trigger gap optimization	mostly Multi
635 - 665	8/14/2007	SF6, 32psi, 6.5" elect., 0.34" gap, TG 0.45"	avg # = 2.8
666 - 674	8/23/2007	SF6, 32psi, 6.5" elect., 0.34" gap, 8 straps	avg # = 2.44
675 - 683	8/23/2007	SF6, 32psi, 6.5" elect., 0.34" gap, 4 straps	avg # = 2.44
684 - 695	8/24/2007	SF6, 32psi, 6.5" elect., 0.34" gap, 8 L1	avg # = 2.67
696 - 707	8/25/2007	SF6, 32psi, 6.5" elect., 0.34" gap, 4 L1	avg # = 2.0
708 - 716	8/27/2007	SF6, 32psi, 6.5" elect., 0.34" gap, 8 L2	avg # = 1.5
717 - 736	8/28/2007 - 8/29/07	SF6, 32psi, 6.5" elect., 0.34" gap, 4 L2	avg # = 1.3
737 - 745	8/30/2007	SF6, 32psi, 6.5" elect., Tilt 0.34/0.26, 8 straps	avg # = 1.25
746 - 754	9/5/2007	SF6, 32psi, 6.5" elect., Tilt 0.34/0.30, 8 straps	avg # = 2.33
755 - 763	9/6/2007	SF6, 32psi, 6.5" elect., Tilt 0.34/0.32, 8 straps	avg # = 2.67
764 - 772	9/6/2007	SF6, 32psi, 6.5" elect., Tilt 0.34/0.33, 8 straps	avg # = 2.33
773 - 781	9/7/2007	SF6, 32psi, 6.5" elect., Tilt 0.34/0.26, 8 straps	avg # = 2.56
782 - 790	9/13/2007	SF6, 32psi, 1.5" elect., 0.34" gap, 8 tube	avg # = 1.9
791 - 813	9/17/07 - 9/18/07	SF6, 32psi, 11.5" elect., 0.34" gap, 8 tube	avg # = 6.1
814 - 831	9/19/07 - 9/20/07	SF6, 32psi, 11.5" elect., 0.69" gap, 8 tube	avg # = 3.1
832 - 867	9/20/2007	SF6, 32psi, 11.5" elect., 0.17" gap, 8 tube	avg # = 3.9
868 - 885	9/21/2007	SF6, 32psi, 5.5" elect., 0.34" gap, 8 tube	avg # = 2.9
886 - 903	9/24/2007	SF6, 32psi, 5.5" elect., 0.17" gap, 8 tube	avg # = 3.0
904 - 921	9/25/2007	SF6, 32psi, 5.5" elect., 0.68" gap, 8 tube	avg # = 1.6

Table 6. Summary of experiments conducted on MCST.

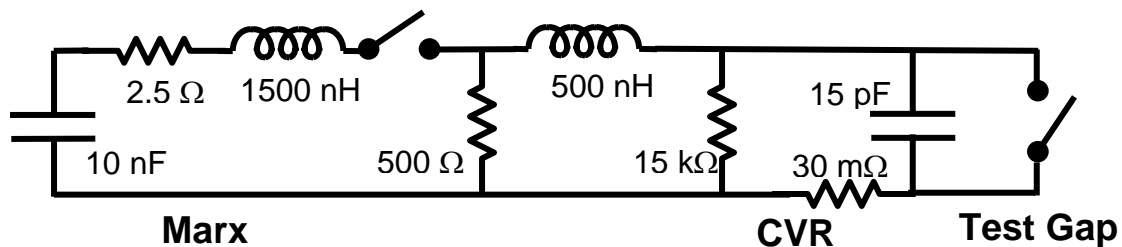


Figure 16. Circuit diagram of MCST has configured in initial tests.



Figure 17. Photo of a 2 channel breakdown (double) from an early shot on MCST.

Brass straps connecting the top of the PG to the test chamber HV feed plate. The HV stalk is mounted to the center of this plate and rises into the test chamber above



Marx

Marx output connected to the bottom of the PG

Peaking Gap (PG)

Figure 18. Photo taken through the MCST tank front port showing the PG installation.

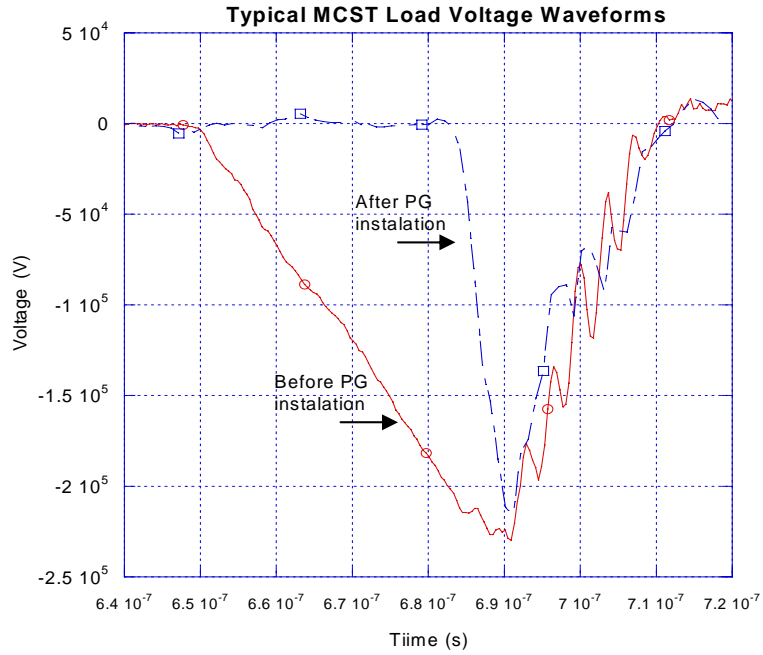


Figure 19. Typical MCST load voltage waveforms before and after PG installation.

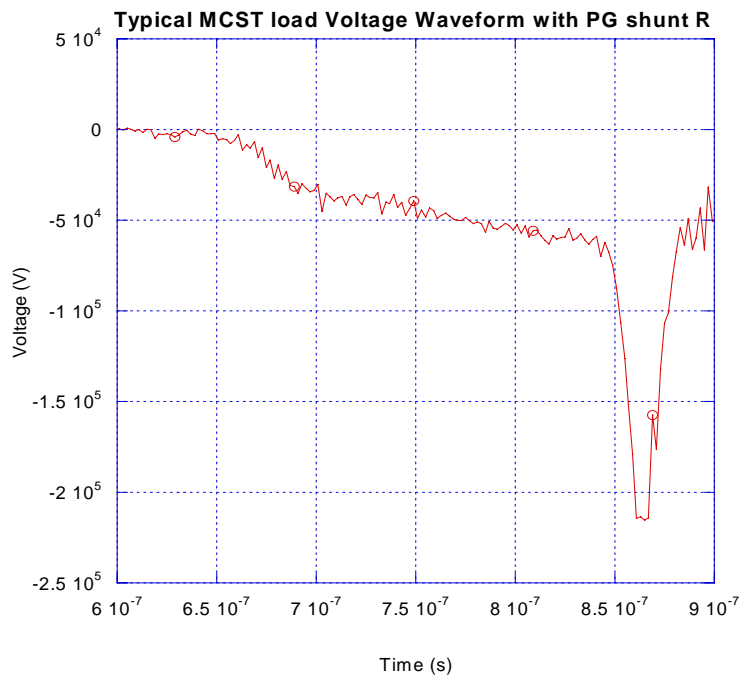


Figure 20. Typical load voltage waveform with a 15 kΩ shunt resistor across the PG.

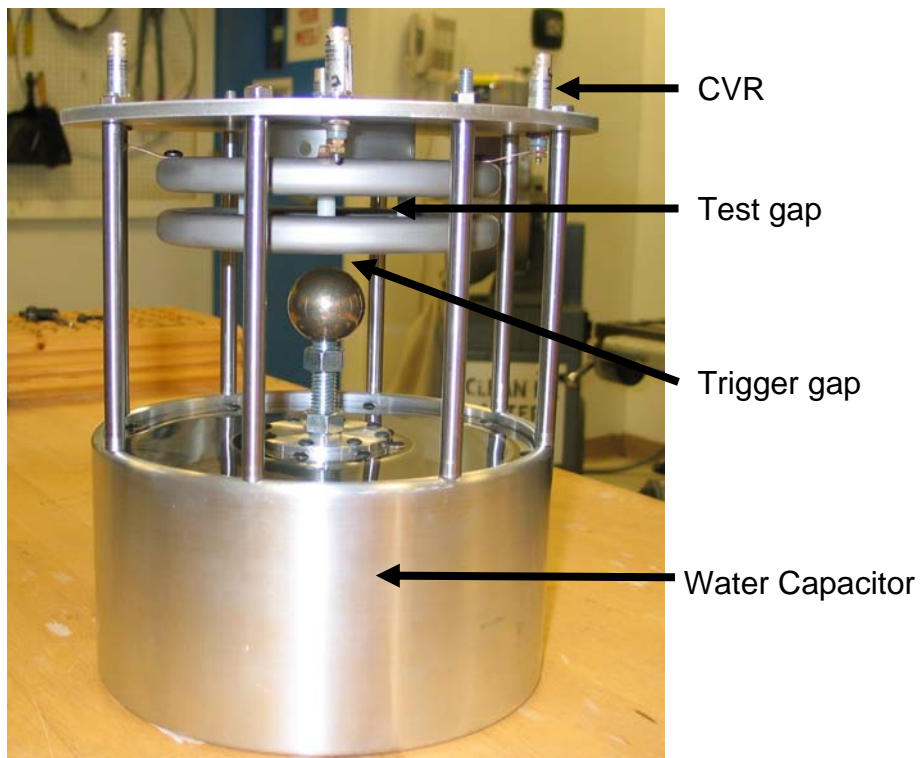
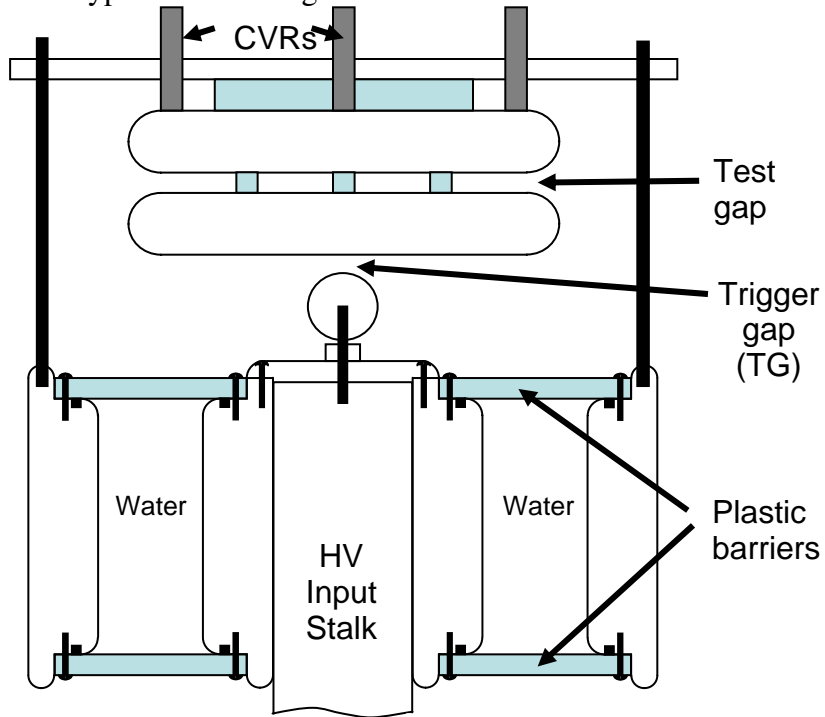


Figure 21. Cross-section drawing and photo of the water capacitor test assembly.

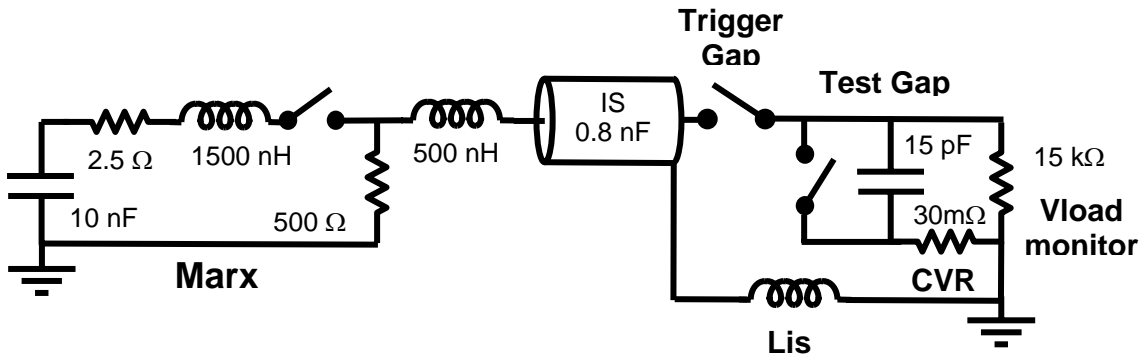


Figure 22. Circuit diagram of MCST with reconfigured test assembly including a water capacitor (IS) and a trigger gap.

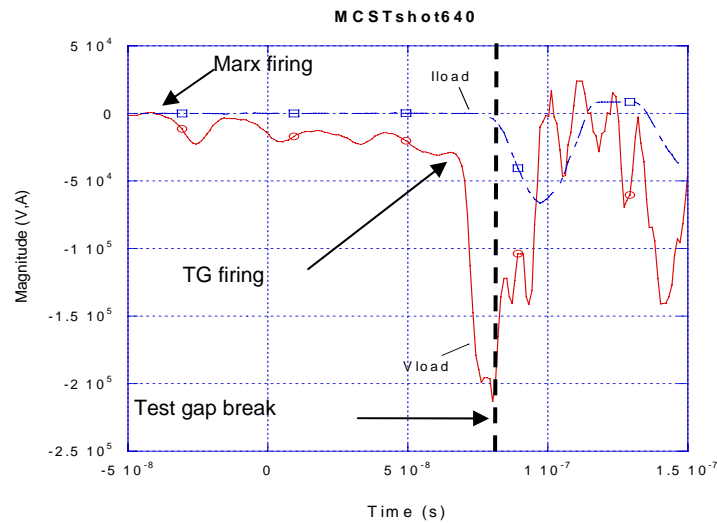


Figure 23. Load voltage and current waveforms from MCST shot # 640 which was a 5 channel breakdown shot.



Figure 24. Photo of the 5 channel breakdown on MCST shot 640.

#### IV. Results of MCST Experiments

With consistent multi-channel behavior finally achieved, the balance of the time on the LDRD was devoted to scanning key parameters and recording the effect on multi-channel behavior. The performance exhibited by the new setup seemed to confirm that source impedance was a key parameter, so, the first parameter scan conducted was on source impedance. A convenient way to increase the effective source impedance in the new setup was to increase the inductance of the connection between the outer shell of the water IS and ground ( $L_s$  in the circuit diagram of Fig. 22). In Fig. 25, two higher inductance implementations are shown. In the original water IS setup (Fig. 21), the top/ground plate is supported by 8 stainless steel tubes which also serve as the electrical connection to the IS outer shell. In the setups of Fig. 25, the stainless tubes have been replaced with plastic tubes and the electrical connection is 8 copper wire straps (top photo) and 8 copper wire coils (bottom photo,  $L_1 = 1.2 \mu\text{H}$  each). In the impedance scan test series, the goal was to incrementally increase the inductance until multi-channeling was rare event (as is was in the earliest MCST tests). In this series, 6.5" diameter electrodes with the nominal 0.34" gap and 32 psi pressure was used in all 7 configurations. An estimate for the inductance of each configuration was calculated using Grover[7] as shown in Fig. 26. The purpose of the calculation was to estimate the inductance external to the test gap to use in the calculation of an effective source impedance;

$$Z = \sqrt{L / C} .$$

The inductances of the 7 configurations ranged from 67nH in the 8 x tubes case up to 681nH in the 4 x L2 case which yielded an impedance range of 9 to 29  $\Omega$ . For comparison the impedance of the ZR IS is  $\sim 4 \Omega$ . The results of the impedance scan tests are tabulated and plotted in Fig 27. With the limited time available for these tests, only on the order of 10 shots were taken on each configuration and the standard deviations for each data set seemed to be high (>30 % typically). However, the data does indicate a definite downward trend in the average # of channels as circuit impedance increases as shown in Fig. 27.

Before moving to the electrode diameter test series, a quick series was conducted to assess the importance of gap spacing tolerances on multi-channel behavior. The question was; how tight would gap tolerances need to be maintained in larger diameter electrodes so that results were not tainted by gap tilt. A photo of the setup for this test series along with the results are shown in Fig. 28. In this series, 6.5" diameter electrodes with 32 psi pressure and 8 x copper straps were used. The gap was purposely tilted as shown in the photo so that the gap spacing on one side was long and the other side was short (Tilt = long gap - short gap). The long gap was set at the nominal 0.34" and the short gap was varied. Four tilt settings (0.01", 0.02", 0.04", and 0.08") were tested. The data from the test are tabulated in the figure. Over this relatively gross range of tilt the average # of channels per shot was **not** effected. The only significant effect noticed was the preference (as would be expected) for the channels to form on the short side. The plot in Fig. 28, shows how the percentage channels on the long side declines as the tilt increases. When the tilt got to 0.08" no channels were observed on the long side.

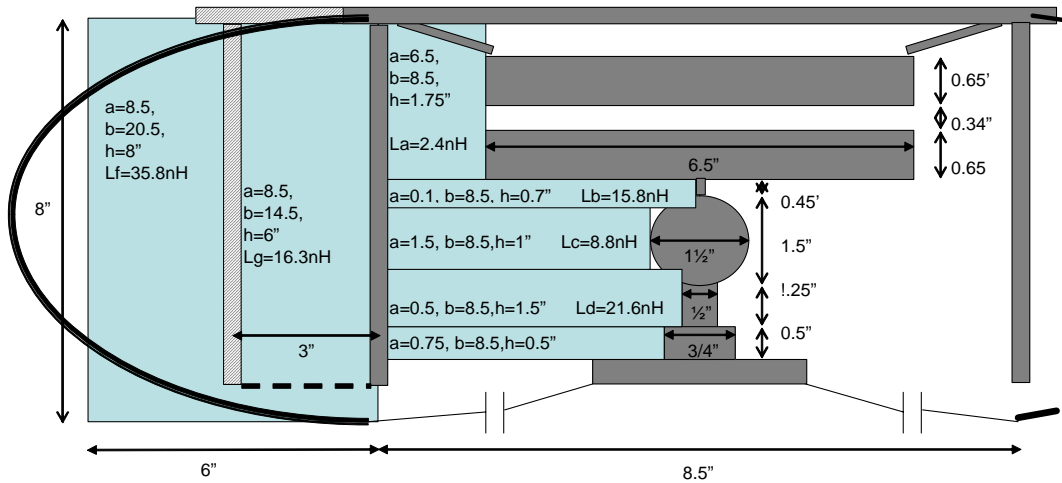
In the electrode diameter test series, the standard 6.5" diameter was tested along with three other diameters (1.5", 5.5", and 11.5 "). These setups are shown in Fig. 29. In this series, a nominal 0.34" gap with 32 psi pressure and 4 x stainless steel tubes were used. The results of these tests are summarized in Fig. 30. The plot of average # of channels per shot shows a definite increasing trend as the electrode diameter is increased. With 11.5" diameter electrodes the average # of channel per shot was > 6. Even though time only permitted on the order of 10 shots per setup and the standard deviations are high (~30%), the trend seems real. This result seems to give a very positive answer the key technical question of interest in phase II of this LDRD. **Multi-channel behavior would likely be enhanced in an LTS cascade section of greater diameter.** This suggests that low inductance switch concept developed in phase I of this LDRD would be a viable option and it would be reasonable to take the development of the concept to the next level by building a proof of concept switch to test.

In the few days remaining on the LDRD a final quick test series was conducted in which the gap spacing was varied off the nominal. In this series, the 5.5" and 11.5" setups of Fig 29 were used. The gaps were set to half nominal (0.17") and then to twice nominal (0.68"). The results of this series are summarized in Fig. 31. The purpose of these tests was to begin testing in different electric field regimes. With the limited data and analysis possible before the end of the LDRD, no conclusions can be drawn from this data.

As a follow-on to the LDRD work, department 1671 will continue to support the small scale experiments for a few months to complete data collection and data analysis so that a high quality journal paper can be produced. The emphasis of this work will be to expand the data sets that have already been collected to improve the statistics of the experimental data. This will also allow for more detailed analysis which will be directed at deriving expressions that describe the relationships between key parameters and the average # of channels that would be expected in a cascade type spark gap. Preliminary work in this area is already in progress. L3 Communications was commissioned in the last year of the LDRD to a literature search of previous work and begin developing expressions to characterize multi-channel behavior. A report [8] summarizing this effort has been delivered.



Figure 25. Photos of experimental setups where inductance was added to increase circuit impedance. The top photo shows the 8 x straps setup and the bottom photo shows the 8 x L1 setup.



La1 =	h = 1.75 15.4206	b = 8.5 nH	a = 1.5	La11 =	h = 1.75 -2.68728	b = 8.5 nH	a = 11.5	Ld =	h = 1.5 21.58909	b = 8.5 nH	a = 0.5
La5 =	h = 1.75 3.869978	b = 8.5 nH	a = 5.5	Lb =	h = 0.7 15.79807	b = 8.5 nH	a = 0.1	Le =	h = 0.5 6.166481	b = 8.5 nH	a = 0.75
La6 =	h = 1.75 2.384867	b = 8.5 nH	a = 6.5	Lc =	h = 1 8.811773	b = 8.5 nH	a = 1.5	Lf =	h = 8 35.77778	b = 20.5 nH	a = 8.5
				Lg =	h = 6 16.27883	b = 14.5 nH	a = 8.5				

**Calculating the base inductance assuming solid conductor shells**

L0 = La+Lb+Lc+Ld+Le = 54.75027 nH with tubes  
 L0 = La+Lb+Lc+Ld+Le+Lf = 90.52805 nH with straps

L01.5"= 84.06484  
 L05.5"= 72.51422  
 L011.5"= 65.95696

**Calculating correction terms using Grover pg 43 eq. #27**

N=# wires, p=wire dia.

L(nH) =	Base (L0)	+	Correction1 (Lc1)	+	Correction2 (Lc2)	+	Correction3 (Lc3)
L(nH) =	200h Ln(b/a)	+	200h( Ln (b/Np) )/N	+	200h(0.25)	+	200h/(4N)

	Lcoil	N	b	p	h	L0	Lc1	Lc2	Lc3	Ltot
<b>8 tubes</b>	0	8	8.5	0.375	6	54.75027	3.967939	7.62	0.9525	67.29071
<b>8 straps</b>	0	8	20.5	0.125	8	90.52805	15.34376	10.16	1.27	117.3018
<b>4 straps</b>	0	4	20.5	0.125	8	90.52805	37.72989	10.16	2.54	140.9579
<b>8 L1</b>	1200	8	20.5	0.125	8	90.52805	15.34376	10.16	1.27	267.3018
<b>4 L1</b>	1200	4	20.5	0.125	8	90.52805	37.72989	10.16	2.54	440.9579
<b>8 L2</b>	2160	8	20.5	0.125	8	90.52805	15.34376	10.16	1.27	387.3018
<b>4 L2</b>	2160	4	20.5	0.125	8	90.52805	37.72989	10.16	2.54	680.9579
<b>4 tube1.5"</b>	0	4	14.5	0.375	6	84.06484	17.28737	7.62	1.905	110.8772
<b>4 tube5.5"</b>	0	4	14.5	0.375	6	72.51422	17.28737	7.62	1.905	99.32659
<b>4 tube11.5"</b>	0	4	14.5	0.375	6	65.95696	17.28737	7.62	1.905	92.76933

Figure 26. Drawing and spreadsheet showing how inductances for the various setups was estimated.

parameter scanned Lis

gap = 0.34 dia. = 6.5" press = 32 psi

descript.	L est.	avg# ch.	st. dev.	Ndata	Zest	avg# ch.
8xtubes	67.290714	2.88	1.05	17	9.171335	2.88
8xstraps	117.30181	2.44	0.53	9	12.10897	2.44
4xstraps	140.95794	2.38	0.52	9	13.27394	2.38
8xL1	267.30181	2.73	0.65	11	18.27915	2.73
4xL1	440.95794	2.00	0.71	9	23.47759	2.00
8XL2	387.30181	1.50	0.53	8	22.00289	1.50
4xL2	680.95794	1.31	0.48	16	29.17529	1.31

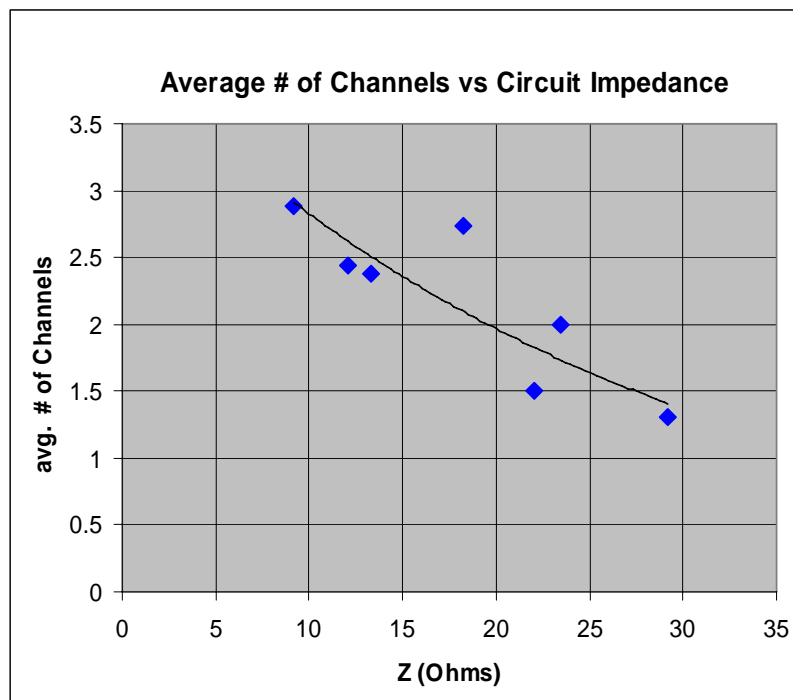
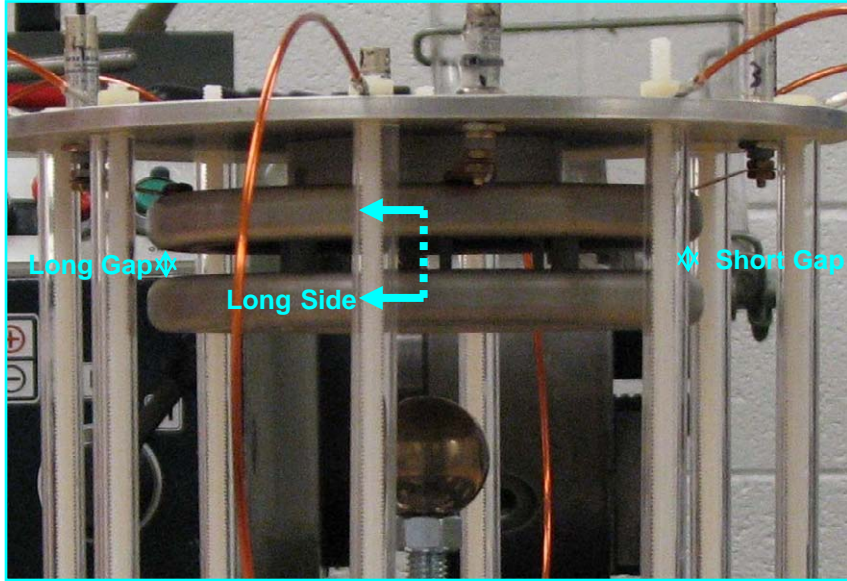


Figure 27. Data and plot showing how the average # of channels declines as circuit impedance increases.



parameter scanned	Tilt
L est. = 117nH	dia. = 6.5"      press = 32 psi

descript.	gap (")	Tilt (")	%chs on left	avg# ch.	st. dev.	Ndata	Zest
8xstraps	0.34/0.26	0.08	0	2.56	0.73	9	12
8xstraps	0.34/0.30	0.04	17	2.33	0.50	9	12
8xstraps	0.34/0.32	0.02	25	2.67	0.70	9	12
8xstraps	0.34/0.33	0.01	43	2.33	1.00	9	12

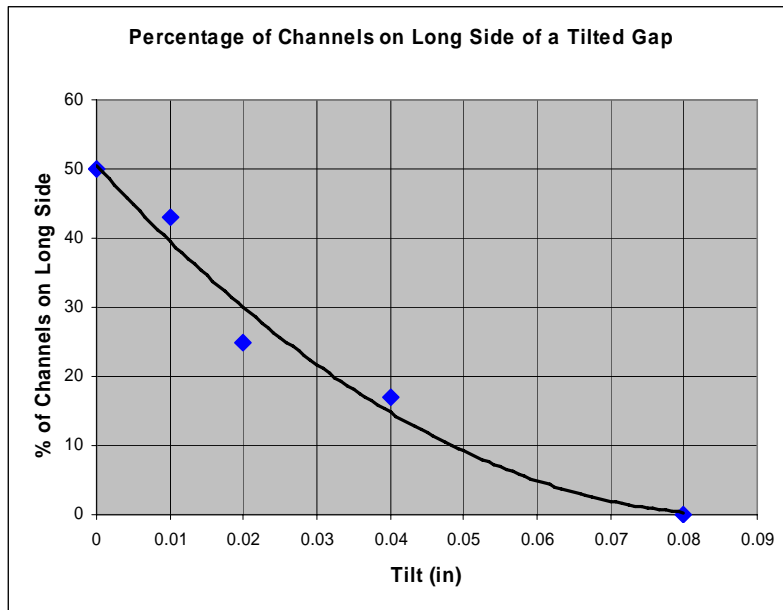


Figure 28. Photo, data, and plot from the gap tilt experiments.



Experimental setup with 1.5" diameter



Experimental setup with 5.5" diameter



Experimental setup with 11.5" diameter

Figure 29. Photos of the setups with 1.5", 5.5", and 11.5" diameter electrodes.

parameter scanned diameter

gap = 0.34 press = 32 psi

descript.	L est.	dia.(")	avg# ch.	st. dev.	Ndata	Zest
4xtubes	111	1.5	2.13	0.83	8	12
4xtubes	99	5.5	2.88	0.89	16	11
8xtubes	67	6.5	2.88	1.05	17	9.2
4xtubes	93	11.5	6.10	1.50	21	11

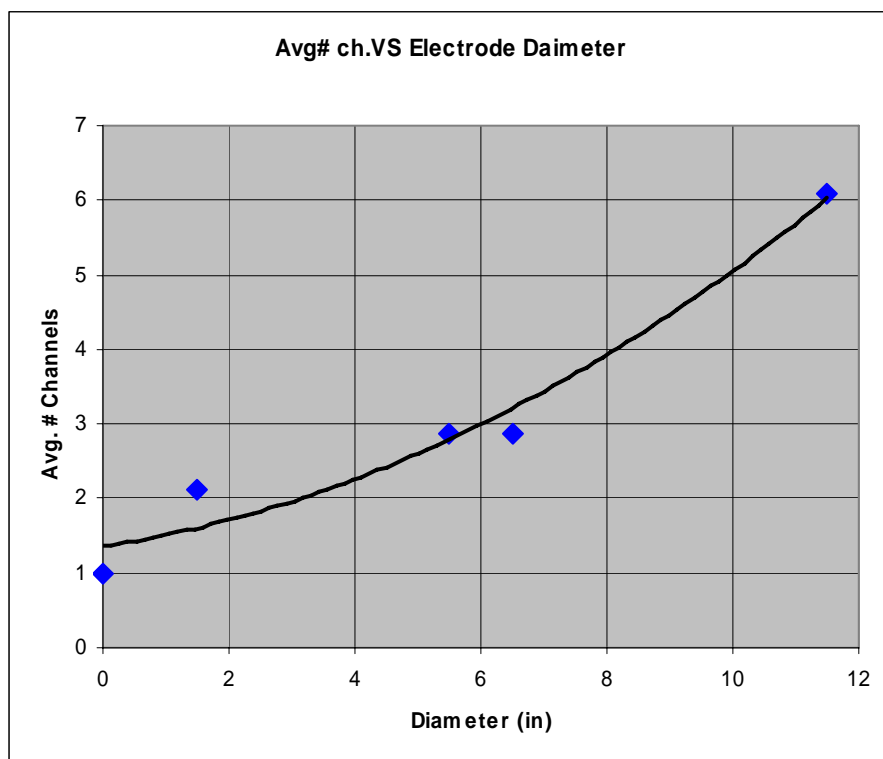


Figure 30. Data and plot from electrode diameter experiments showing how the average # of channels increases significantly as electrode diameter increases.

parameter scanned gap

diameter = 5.5" press = 32 psi

descript.	L est.	gap. (")	avg# ch.	st. dev.	Ndata	Zest
4xtubes	99	0.17	3.00	0.52	16	11.1243
4xtubes	99	0.34	2.88	0.89	16	11.1243
4xtubes	99	0.68	1.60	0.91	15	11.1243

diameter = 11.5" press = 32 psi

descript.	L est.	gap. (")	avg# ch.	st. dev.	Ndata	Zest
4xtubes	93	0.17	3.88	1.14	34	10.78193
4xtubes	93	0.34	6.10	1.50	21	10.78193
4xtubes	93	0.69	3.11	1.68	18	10.78193

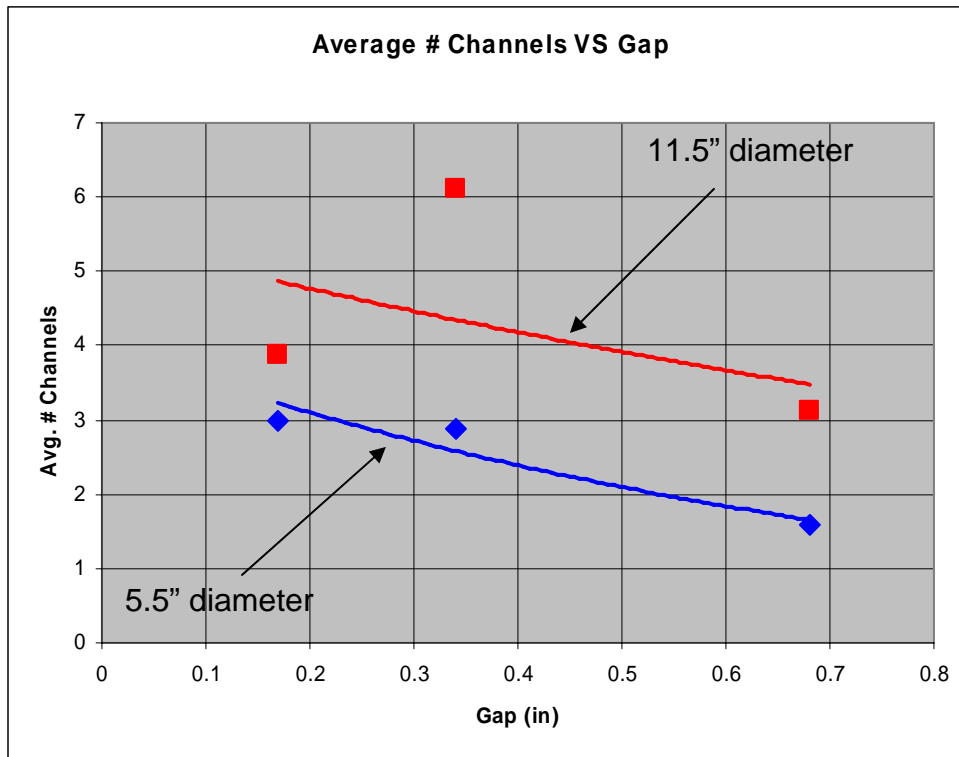


Figure 31. Data and plot from preliminary gap separation experiments showing how the average # of channels varies with gap spacing. More data and analysis is required to draw conclusions from these experiments.

## V. SUMMARY

The laser trigger switch (LTS) is a key component in ZR-type pulsed power systems. In ZR, the pulse rise time through the LTS is  $> 200$  ns and additional stages of pulse compression are required to achieve the desired  $< 100$  ns rise time. Water switches are currently used to do the balance of the pulse compression and water switches have several undesirable characteristics; they introduce significant timing jitter, they are relatively lossy, and they generate destructive mechanical shock waves upon closure. Each of these features worsens as the water switch is required to do more pulse compression. For these reasons, there is much to be gained by reducing the work the water switches have to do or perhaps eliminating a stage completely.

The inductance of the LTS in large part determines what the energy transfer time through the switch is and the ZR LTS has an inductance of  $\sim 500$  nH. The current path through the cascade section of the ZR LTS is at a diameter of  $\sim 6$ " which is certainly not optimal from an inductance point of view. The LTS connects components of much greater diameter (typically 4'-5'). In this LDRD the viability of switch concepts in which the diameter of cascade section is greatly increased have been investigated. The key technical question to be answered was, will the desired multi-channel behavior be maintained in a cascade section of larger diameter.

The LDRD proceeded in 2 distinct phases. The original plan for the LDRD was to develop a promising switch concept and then design, build, and test a moderate scale switch which would demonstrate the key features of the concept. In phase I, a switch concept which meet all electrical design criteria and had a calculated inductance of 150 nH was developed. In this concept the oil envelope around the switch was eliminated and a hybrid trigger section is used. The cascade electrodes were pushed to larger diameters and the diameters of the individual cascade electrodes were varied along the length of the switch. In addition the electrode gap spacings were allowed to vary along the length of the switch. In this way, uniform field grading in the cascade gaps was achieved without having to include a large field shaper.

To test and demonstrate the key features of this concept, a 1.5 MV test switch was designed and fabrication was initiated. In the design effort, the details of manufacture, assembly, and operation were thoroughly examined and the necessary tradeoffs were negotiated. At the end of the process, confidence was high that the switch would be both mechanically and electrically sound. The LDRD was then redirected due to budgetary concerns. The fabrication of the switch was halted and the focus of the LDRD was shifted to answering the key technical question concerning multi-channel behavior in a smaller scale experiment.

In phase II, the Multi-channel switch test bed (MCST) was designed and constructed. The purpose of MCST was to provide a versatile, fast turn around facility for the study the multi-channel electrical breakdown behavior of a ZR type cascade switch gap in a parameter space near that of a ZR LTS. Achieving consistent multi-channel behavior in small test bed like MCST turned out to be challenging because the impedance of the source was too high and source impedance was found to be a key parameter for multi-channeling. Parameter scans on source impedance, gap tilt, gap spacing and electrode diameter were conducted. In the standard gap (6.5" dia., 32 psi SF6, 0.34" gap), the average # of channels observed per shot was 2.88. Under similar

conditions with 11.5” diameter electrodes, the average # of channels observed per shot was 6.1.

**These experiments clearly indicate that multi-channel behavior is enhanced by increasing electrode diameter.** This is a positive answer to the one remaining technical question concerning the viability of the low inductance switch concept developed in phase I of this LDRD. The results of this LDRD would support taking the development of the concept to the next level and building a proof of concept switch to test.

## VI. REFERENCES

1. Savage, M., et al., "An Overview of Pulse Compression and Power Flow in the Upgraded Z Pulsed Power Drivers," Proceedings of the 16<sup>th</sup> IEEE Pulsed Power Conference, Albuquerque, NM, 1997.
2. Elizondo, J., et al., "PITHON Water switch experiments jitter fit," ZR Technical Note # 16, April, 2002.
3. Elizondo, J., et al., hybrid trigger switch.
4. K.R. LeChien, J.M. Gahl, et. al, "Development of a Terawatt Test Stand at the University of Missouri for Fast, Multichannel Switching Analysis", 14 IEEE Pulsed Power Conference, Dallas Texas, June, 2003, pp. 1051-1053.
5. Garde, J. internal SNL email, 8-15-2007.
6. Rosenthal, S., et al., "Modeling 6-MV Gas Switches for the ZR Accelerator," 14 IEEE Pulsed Power Conference, Dallas Texas, June, 2003, p. 163.
7. Grover, F., Inductance Calculations, Dover Publications, Inc., New York, 1973.
8. Smith, I. Et al., "Channel Number Predictions for Rimfire Gas Switches," L3 Communications, Final Report for SNL contract # 72991, September, 2007.

## DISTRIBUTION

1	MS1194	Chuck Harjes, 1671
1	MS1194	Ken Struve, 1671
1	MS1194	Mark Savage, 1671
1	MS1194	Bill Stygar, 1671
1	MS0878	Juan Elizondo, 2735
1	MS1193	Ray Chavez, 1645
1	MS1152	Zach Wallace, 1653
1	MS0899	Technical Library, 9536